JAMES | Journal of Advances in Modeling Earth Systems

RESEARCH ARTICLE
10.1029/2018MS001483

Coccolithophore Growth and Calcification in an Acidified Ocean: Insights From Community Earth System Model Simulations

K. M. Krumhardt[1,2], N. S. Lovenduski[3], M. C. Long[2], M. Levy[2], K. Lindsay[2], J. K. Moore[4], and C. Nissen[5]

[1]Environmental Studies Program and Institute of Arctic and Alpine Research, University of Colorado Boulder, Boulder, CO, USA, [2]Climate and Global Dynamics, National Center for Atmospheric Research, Boulder, CO, USA, [3]Department of Atmospheric and Oceanic Sciences and Institute of Arctic and Alpine Research, University of Colorado Boulder, Boulder, CO, USA, [4]Department of Earth System Science, University of California, Irvine, CA, USA, [5]Institute for Biogeochemistry and Pollutant Dynamics, ETH Zürich, Zürich, Switzerland

Key Points:
- An explicit coccolithophore representation in a major Earth System Model is described
- Increasing CO_2 stimulates coccolithophore growth in certain regions, but calcification is impaired
- Future CO_2 conditions drive a decrease in global marine calcium carbonate production

Supporting Information:
- Supporting Information S1

Correspondence to:
K. M. Krumhardt,
kristen.krumhardt@colorado.edu

Citation:
Krumhardt, K. M., Lovenduski, N. S., Long, M. C., Levy, M., Lindsay, K., Moore, J. K., & Nissen, C. (2019). Coccolithophore growth and calcification in an acidified ocean: Insights from community earth system model simulations. *Journal of Advances in Modeling Earth Systems*, *11*, 1418–1437. https://doi.org/10.1029/2018MS001483

Received 21 AUG 2018
Accepted 5 MAR 2019
Accepted article online 12 MAR 2019
Published online 22 MAY 2019

Abstract Anthropogenic CO_2 emissions are inundating the upper ocean, acidifying the water, and altering the habitat for marine phytoplankton. These changes are thought to be particularly influential for calcifying phytoplankton, namely, coccolithophores. Coccolithophores are widespread and account for a substantial portion of open ocean calcification; changes in their abundance, distribution, or level of calcification could have far-reaching ecological and biogeochemical impacts. Here, we isolate the effects of increasing CO_2 on coccolithophores using an explicit coccolithophore phytoplankton functional type parameterization in the Community Earth System Model. Coccolithophore growth and calcification are sensitive to changing aqueous CO_2. While holding circulation constant, we demonstrate that increasing CO_2 concentrations cause coccolithophores in most areas to decrease calcium carbonate production relative to growth. However, several oceanic regions show large increases in calcification, such the North Atlantic, Western Pacific, and parts of the Southern Ocean, due to an alleviation of carbon limitation for coccolithophore growth. Global annual calcification is 6% higher under present-day CO_2 levels relative to preindustrial CO_2 (1.5 compared to 1.4 Pg C/year). However, under 900 μatm CO_2, global annual calcification is 11% lower than under preindustrial CO_2 levels (1.2 Pg C/year). Large portions of the ocean show greatly decreased coccolithophore calcification relative to growth, resulting in significant regional carbon export and air-sea CO_2 exchange feedbacks. Our study implies that coccolithophores become more abundant but less calcified as CO_2 increases with a tipping point in global calcification (changing from increasing to decreasing calcification relative to preindustrial) at approximately ~600 μatm CO_2.

Plain Language Summary CO_2 emissions from human activity are inundating the upper ocean causing ocean acidification. Coccolithophores, a widespread type of marine algae that make calcium carbonate shells, may be particularly influenced by ocean acidification. In this study we created a phytoplankton-type representative of coccolithophores in the Community Earth System Model. We performed experiments to explore how ocean acidification from increasing CO_2 affects coccolithophore growth and calcification. We found that, as CO_2 rises, coccolithophores increase in abundance in several oceanic regions, including the North Atlantic, Western Pacific, and parts of the Southern Ocean, due to a carbon fertilization effect on coccolithophore photosynthesis. However, most areas of the ocean showed decreases in coccolithophore calcification as CO_2 increases and ocean acidification becomes more severe. We project that end-of-the-century CO_2 concentrations result 11% less oceanic calcification on a global scale relative to preindustrial CO_2 levels. Overall, coccolithophores become more abundant in certain regions but are more lightly calcified with increasing CO_2.

1. Introduction

Coccolithophores are the most abundant calcifying phytoplankton in the ocean. Ubiquitous from subpolar waters to the tropics, coccolithophores comprise a substantial fraction of phytoplankton communities throughout many areas of the ocean (Balch et al., 2007; Poulton et al., 2007; Thierstein & Young, 2004). These primary producers exert a unique influence on the global carbon cycle by way of their ability to perform both

calcification and photosynthesis. Through the process of photosynthesis, coccolithophores convert aqueous carbon dioxide (CO_2) to organic matter. Via calcification, coccolithophores take up bicarbonate (HCO_3^-) and calcium ions to precipitate calcium carbonate ($CaCO_3$), decreasing seawater alkalinity and increasing CO_2. Coccolithophores can therefore influence both the biological carbon pump and the alkalinity pump (i.e., the carbonate counter pump, the oceanic production and export of $CaCO_3$). Coccolithophores account for between 1% and 20% of the phytoplankton carbon pools in diverse ocean regions (Jin et al., 2006; Poulton et al., 2007), are responsible for ~10% of carbon export (Jin et al., 2006), and comprise a major fraction of carbonate in the sediments (ranging from 30% to 90%; Broecker & Clark, 2009). The balance between coccolithophore photosynthesis and calcification could be important for ocean carbon cycle processes, such as air-sea CO_2 gas exchange and ballasting organic matter to the deep ocean, especially in regions of dense coccolithophore blooms and oligotrophic waters where coccolithophores can be a substantial portion of the phytoplankton community (Poulton et al., 2007). Changes in coccolithophore photosynthesis and calcification from ocean acidification (OA) would not only impact regional plankton ecology but could also influence how carbon moves from the atmosphere into the surface ocean, and finally to the deep sea.

Coccolithophores have been the focus of numerous laboratory studies due to their potential susceptibility to OA, but these have yielded contradictory results (e.g., Bach et al., 2013; Findlay et al., 2011; Iglesias-Rodriguez et al., 2008; Riebesell et al., 2000; Sett et al., 2014). While some demonstrate decreasing calcification (Riebesell et al., 2000), others show a stimulation of coccolithophore growth and/or no effect on overall calcification (e.g., Iglesias-Rodriguez et al., 2008; Rost et al., 2003). Recent efforts have made progress to reconcile these contradictions by using a "substrate-inhibitor" concept (HCO_3^-/H^+) regarding calcification (Bach, 2015; Bach et al., 2015) or by modeling biochemical reactions inside coccolithophore cells, compartmentalizing intracellular calcification, and photosynthesis from extracellular environmental influences (Furukawa et al., 2018). These studies resolved that culturing conditions, such as the way CO_2 is manipulated, can help to explain differences in experimental results. Further, a large, across-species data compilation recently resolved that coccolithophores generally tend to calcify less relative to photosynthesis as CO_2 increases (Krumhardt et al., 2017a). Photosynthesis by some coccolithophores has been shown to be carbon limited, however, even at today's CO_2 concentrations (in contrast to other phytoplankton, which have more efficient carbon concentrating mechanisms; Krumhardt et al., 2017a; Riebesell, 2004; Rost et al., 2003), indicating that coccolithophore photosynthesis could respond positively to increased CO_2 availability. Therefore, additional CO_2 in the water column could have competing effects on coccolithophore physiological function: (1) photosynthesis in coccolithophores could be stimulated, but (2) coccolithophore calcification could be hindered. These contrasting effects complicate future projections of marine calcification by coccolithophores.

On a global scale, predicting the effects of increasing anthropogenic CO_2 on coccolithophores is important for estimating changes in total global upper ocean calcification and to assess the potential for these changes in calcification to affect other critical carbon cycle processes. On regional scales, changes in phytoplankton resulting from OA could affect marine ecosystems and regional biogeochemistry. A suitable tool for evaluating these potential effects is an Earth System Model with an explicit parameterization for coccolithophores. However, none of the Earth System Models participating in the 5th Coupled Model Intercomparison Project (CMIP5) represent a coccolithophore phytoplankton functional type (PFT) that is sensitive in growth and calcification to changing ocean carbonate chemistry. In this study, we describe a novel explicit coccolithophore parameterization in a state-of-the-art Earth System Model, the Community Earth System Model (CESM) version 2.0.

A number of studies have modeled pelagic calcifiers, such as coccolithophores, on global (e.g., Gregg & Casey, 2007; Heinze, 2004) and regional (e.g., Southern Ocean; Nissen et al., 2018) scales. Some have aimed to quantify the sensitivity of the global carbon cycle to changes in pelagic calcification using global models in which the net $CaCO_3$ production or dissolution is sensitive to the $CaCO_3$ saturation state (Ω; e.g., Gangstø et al., 2011; Gehlen et al., 2007; Kvale et al., 2015a, 2015b; Pinsonneault et al., 2012; Ridgwell et al., 2007). Indeed, these modeling studies found that including the influence of changing carbonate chemistry on the production and/or dissolution of $CaCO_3$ fosters important climate-carbon feedbacks in the Earth system. Decreases in calcification from OA result in an additional oceanic CO_2 uptake from the atmosphere of between 6 and ~25 Pg C by the year 2100, with much of the uncertainty stemming from various responses of pelagic calcifiers to OA (Ridgwell et al., 2007, 2009). However, the biogeochemical response to

decreasing calcification may have only a small impact on global atmospheric CO_2 compared to total anthropogenic emissions and other climate-carbon feedbacks (Heinze, 2004; Pinsonneault et al., 2012; Ridgwell et al., 2009). Here we test this conclusion and build upon these previous studies by parameterizing an across-species coccolithophore PFT in a state-of-the-art Earth System Model. This parameterization is unique in that growth rate and calcification are sensitive to changing aqueous CO_2 content. Further, the growth and calcification of the coccolithophore PFT can be modified by temperature and nutrient limitation as described by Krumhardt et al. (2017a). The main goal of this work is to assess global- and regional-scale impacts of increasing CO_2 on coccolithophores, to evaluate the influence of these impacts on phytoplankton community structure, and to examine how these changes could affect important carbon cycle processes, such as carbon export and air-sea CO_2 exchange.

Here we perform sensitivity studies with our novel model configuration to explore how coccolithophore growth and calcification may change under increasing atmospheric CO_2. We isolate the effects of increasing CO_2 by running CESM simulations under various levels of atmospheric CO_2 while holding climate constant: preindustrial (285 μatm), modern (400 μatm), two midcentury concentrations (600 and 700 μatm), and an end-of-the-century high-concentration value (900 μatm). These experiments demonstrate that increasing atmospheric CO_2 stimulates coccolithophore growth but decreases coccolithophore calcification. Relative to the preindustrial control, these counteracting responses lead to a net increase in global pelagic $CaCO_3$ production under 400 μatm CO_2 and a net decrease under 900 μatm CO_2, with near-zero net change in global calcification at 600 μatm CO_2.

2. Methods

2.1. An Explicit Coccolithophore Parameterization in CESM

The marine ecosystem in CESM is simulated using the Marine Biogeochemical Library (MARBL; for documentation see https://marbl-ecosys.github.io/). The flexible structure of MARBL facilitates the addition of novel zooplankton and phytoplankton PFTs in CESM. The current study uses a prerelease version of CESM 2.0 (CESM2; the physical ocean model and ocean ecosystem model are the same as the released version) with a modified version of MARBL that contains explicit coccolithophores. This version of MARBL was modified from the original MARBL, which is based on the three PFT version of the biogeochemical elemental cycling (BEC) model (described in Moore et al., 2002, 2004, 2013). The BEC model is a marine ecosystem model used in previous versions of CESM, representing major phytoplankton groups, limiting macronutrients, iron cycling, and organic matter (as well as biomineral ballast) in the ocean. CESM2 includes a modified Q10 growth parameterization (Sherman et al., 2016) and improvements to the treatment of dissolved organic matter cycling (Letscher et al., 2015).

CESM-cocco includes four PFTs; ecologically relevant parameters are listed in Table 1 (compare to Moore et al., 2002, 2004). Model parameters were tuned using various observational data sets on phytoplankton biomass (Buitenhuis et al., 2013; O'Brien et al., 2016), satellite-derived marine net primary production (Behrenfeld & Falkowski, 1997), nutrients and ocean alkalinity (Lauvset et al., 2016; Locarnini et al., 2013), coccolithophore-associated $CaCO_3$ (Balch et al., 2007), and global estimates of upper ocean calcification (e.g., Feely et al., 2004). Small phytoplankton, diatom, and diazotroph PFTs were carried over from previous versions of CESM; PFTs were carried over from earlier versions, but some parameters have been modified (Table 1; Moore et al., 2002, 2004, 2013). Maximum growth rates are modified by fractional limitation terms for temperature, nutrients, and light (Moore et al., 2002). The nitrogen-fixing "diazotroph" PFT parameterization remained unchanged from previous versions. The parameter values for the "diatom" PFT in CESM-cocco, an explicit silicifier, were slightly modified from previous parameterizations described in Moore et al. (2004). Here, a higher half saturation constant for silicate ($K_{SiO3,diat}$; see parameters in Table 1) was used to increase SiO_3 limitation for the diatoms, helping to open a niche for the coccolithophores; the $K_{SiO3,diat}$ value used in this study is supported by laboratory studies (Paasche, 1973; Sarthou et al., 2005). The "small phytoplankton" PFT is mainly representative of marine cyanobacteria, such as *Prochlorococcus* and *Synechococcus*. This group has the lowest half saturation constants for nutrient uptake of all the PFTs, indicative of competitive fitness in low nutrient regions. In the original BEC model, the small phytoplankton group contained an implicit calcifier fraction, which represented coccolithophores (see Figure S1 in the supporting information for a map of $CaCO_3$ using this previous version; Moore et al., 2004). This functionality was transferred to the explicit calcifier "coccolithophore" PFT in CESM-cocco.

Table 1
List of Relevant Parameterizations Used in CESM2 With Coccolithophores

Parameter	Unit	Definition	cocco	diat	sp	diaz
μ_{max}	day^{-1}	Maximum C-specific growth rate	4.7	5.0	4.4	2.2
α	$\frac{mmol\ C\ m^2}{mg\ Chl\ W\ s}$	Initial slope of photosynthesis-irradiance curve	0.28	0.39	0.35	0.39
Θ_{max}	$\frac{mg\ Chl}{mmol\ N}$	Maximum Chl:N ratio	3.5	4.0	2.5	2.5
K_{Fe}	$\mu mol/m^3$	Fe half saturation constant	0.0315	0.08	0.03	0.045
K_{PO4}	$mmol/m^3$	PO_4 half saturation constant	0.006	0.05	0.005	0.015
K_{DOP}	$mmol/m^3$	DOP half saturation constant	0.25	0.5	0.3	0.1
K_{NO3}	$mmol/m^3$	NO_3 half saturation constant	0.2	0.5	0.2	2
K_{NH4}	$mmol/m^3$	NH_4 half saturation constant	0.01	0.05	0.01	0.2
K_{SiO3}	$mmol/m^3$	SiO_3 half saturation constant	n/a	1.8	n/a	n/a
K_{CO2}	$mmol/m^3$	CO_2 half saturation constant	1	n/a	n/a	n/a
$Z\mu_{max}$	day^{-1}	Maximum zoo grazing rate	2.95	3.41	3.6	3.35
z_{graze}	$mmol/m^3$	Zooplankton grazing half saturation constant	0.854	0.720	0.54	0.600

Note. Abbreviations: small phytoplankton (sp), diatoms (diat), diazotrophs (diaz), coccolithophores (cocco), zooplankton (zoo), and dissolved organic phosphorus (DOP). n/a = not applicable.

The coccolithophore PFT is formulated to be representative of studied coccolithophores, including species from *Syracosphaera* and *Coccolithus* genera, *Calcidiscus leptoporus*, *Gephyrocapsa oceania*, and four distinct morphotypes of *Emiliania huxleyi*. These coccolithophore groups cover most regions of the global ocean and encompass a range of size classes (Krumhardt et al., 2017a). While we cannot accurately represent all niches that different coccolithophore species occupy, the aim is that this single coccolithophore PFT represents coccolithophore biogeography and physiology on the basis of current knowledge. Relationships between coccolithophore growth rate/calcification and temperature, nutrients, and CO_2 were parameterized based on a large data compilation (the majority of studies contributing to this compilation are based on *Emiliania huxleyi*, the most widespread coccolithophore species; Krumhardt et al., 2017a). This PFT is prescribed a low initial slope of the photosynthesis-irradiance curve (α_{cocco}), necessary to restrict blooms in subpolar regions to the summer months, when light is most plentiful. Coccolithophores are the only PFT that can be limited by CO_2 in the model (Riebesell, 2004; Rost et al., 2003). CO_2 is handled as an additional nutrient required for coccolithophore photosynthesis and treated using the same Monod formulation as other nutrients (see K_{CO2} in Table 1). We chose the Monod equation because it has been used in previous studies describing carbon limitation of coccolithophores (Riebesell, 2004; Rivero-Calle et al., 2015; Rost et al., 2003) and it captures the organic carbon-based growth rates summarized in Krumhardt et al. (2017a). We note that the Monod equation ignores the negative effect on growth at high CO_2 concentrations when calcification may be greatly reduced (see sections 4.2 and 4.4). The parameterization for carbon limitation of coccolithophores was treated conservatively: we used a K_{CO2} of 1 $mmol/m^3$, the lower limit of derived K_{CO2} values in Krumhardt et al. (2017a; the mean value was 2.1 $mmol/m^3$), resulting in less carbon limitation of the coccolithophore PFT. Carbon limitation of the coccolithophore PFT mainly occurs in the winter months when all other nutrients required for photosynthesis are abundant (see supporting information).

We applied a power function-based temperature limitation curve for coccolithophores (Krumhardt et al., 2017a), based on results from Fielding (2013) that showed that coccolithophores have a unique temperature-growth rate relationship relative to other phytoplankton:

$$T_{func} = 0.12 \cdot T^{0.4} \quad (1)$$

where T is temperature in degrees Celsius for temperatures between 0 and 27 °C. T_{func} is held constant at temperatures greater than 27 °C. The resulting T_{func} is a fractional value, which is multiplied by the maximum growth rate of coccolithophores (μ_{max}), yielding the temperature-dependent maximum growth rate. All other PFTs use the Q10 temperature parameterization from previous versions of CESM (using a Q10 value of 1.7 and a reference temperature of 30 °C; Sherman et al., 2016). Figure S2 shows a comparison of temperature-dependent growth rates of each PFT. Coccolithophores have lower temperature-limited growth

rates than diatoms and small phytoplankton and cease growth completely at temperatures <0 °C (Holligan et al., 2010).

$CaCO_3$ production by coccolithophores is dependent on temperature, phosphorus limitation, and $CO_{2(aq)}$. We use the ratio of the production of $CaCO_3$ to the production of organic carbon (C) in coccolithophores to convert coccolithophore C-specific growth rates to calcification rates (i.e., $CaCO_3$ production), such that

$$\mu_{CaCO_3} = \mu \cdot r_{CaCO_3:C} \tag{2}$$

where μ_{CaCO_3} is calcification by coccolithophores and μ is C-specific growth rate of coccolithophores (both in units of mol C per unit volume per unit time). Modifications to coccolithophore $r_{CaCO_3:C}$ under varying environmental conditions are described in Krumhardt et al. (2017a; where $r_{CaCO_3:C}$ = coccolithophore particulate inorganic carbon to particulate organic carbon production ratio, PIC/POC). Briefly, coccolithophore $r_{CaCO_3:C}$ decreases linearly as CO_2 increases via the equation:

$$r_{CaCO_3:C} = -0.0136 \cdot CO_{2(aq)} + 1.21 \tag{3}$$

where $CO_{2(aq)}$ is in mmol/m^3. The negative relationship between CO_2 and coccolithophore $r_{CaCO_3:C}$ is supported by meta-analyses of short-term experiments (Findlay et al., 2011; Krumhardt et al., 2017a), long-term culture experiments (Lohbeck et al., 2012), and paleoecological data from the last ~50,000 years (Beaufort et al., 2011). A positive linear function between temperature and $r_{CaCO_3:C}$ for temperatures below 11 °C is used, resulting in low $r_{CaCO_3:C}$ at low temperatures. A fractional P limitation term ($PO_4/(PO_4 + K_{PO4,cocco})$) further modifies $r_{CaCO_3:C}$, resulting in slightly higher $r_{CaCO_3:C}$ values under high P limitation (when the P limitation term is low).

Biological dissolution of $CaCO_3$ in the upper ocean is an important process for maintaining the vertical alkalinity gradient (Barrett et al., 2014; Iglesias-Rodriguez et al., 2002; Milliman et al., 1999; Schiebel, 2002). In the open ocean, biologically mediated $CaCO_3$ dissolution occurs between depths of 100 and 700 m (Schiebel, 2002). At these depths, low pH conditions are created in sinking aggregates, fecal pellets, and decomposing cytoplasm within dead plankton cells, resulting in $CaCO_3$ dissolution in $CaCO_3$-saturated waters (Milliman et al., 1999). This is accounted for in CESM2 with a prescribed remineralization length scale for $CaCO_3$ that is 500 m in the upper ocean. Biological dissolution is more explicitly modeled through the fraction of $CaCO_3$ that is dissolved in zooplankton guts (ν_{ZCaCO3}). A ν_{ZCaCO3} value of 0.7 favors $CaCO_3$ dissolution under environmental conditions that increase zooplankton growth rates (and thus the potential for biologically mediated $CaCO_3$ dissolution).

Remineralization of organic matter at depth is based on the mineral ballast model described by Armstrong et al. (2002) and summarized in Moore et al. (2004). Briefly, POC is divided into soft and hard fractions, with the hard fraction being quantitatively associated with ballast minerals and the soft fraction being the excess POC. Thus, the hard fraction depends on the amount of POC associated with each ballast mineral: 10% of $CaCO_3$ (from coccolithophores) and 10% of biogenic silica (from diatoms) is associated with the hard POC pool, while 98% of dust-associated POC enters the hard POC pool. The hard POC fraction has a long remineralization scale of 40,000 m (thus, e.g., most of hard fraction remains after sinking to 4,000 m of ocean depth), while the excess soft particulate flux sinks with remineralization dependent on composition. POC, silica, and $CaCO_3$ have initial remineralization length scales of 100, 770, and 500 m, respectively, in surface waters. These length scales increase with depth down to 1,000-m depth, with additional increase under low oxygen conditions. The increases in length scale have been optimized to match the global mean PO_4 profile (for POC), and the mean profiles for alkalinity and SiO_3.

One zooplankton group differentially grazes each PFT in CESM-cocco. The small phytoplankton group has the highest maximum grazing rate (see $Z\mu_{max}$ parameters in Table 1). Coccolithophores have the lowest maximum grazing rate following the hypothesis that the coccosphere protects from grazing and viral attack (Monteiro et al., 2016; Olson & Strom, 2002). The diatoms grazing rate is higher than for coccolithophores but also lower than small phytoplankton. The grazing rate of the small phytoplankton PFT follows a sigmoidal grazing curve (Holling type III grazing), allowing lower grazing rates on small phytoplankton at low abundance (e.g., in the oligotrophic gyres). The other three PFTs have prescribed Michaelis-Menten grazing (Holling type II). Both Holling types II and III grazing functions are common in ocean ecosystem modeling

(Irwin & Finkel, 2018; Laufkötter et al., 2016). Specific values for maximum grazing rates and half saturation constants for grazing for each PFT are listed in Table 1.

2.2. CESM Simulations and Analysis

The CESM-cocco simulations described here were generated from an ocean-sea ice configuration of the CESM2.0 that was forced with repeating annual cycles of momentum, heat, and freshwater fluxes (so-called "normal year" forcing; Large & Yeager, 2004). The ocean model in CESM2.0, the Parallel Ocean Program, a level-coordinate ocean general circulation model with 60 vertical levels, was run at the nominal one degree resolution for CESM with displaced pole grid. Ocean temperature and salinity were initialized by World Ocean Atlas version 2 (Locarnini et al., 2013) and Polar Science Center Hydrographic Climatology (Steele et al., 2001); ocean physics were spun up for 100 years to achieve quasi-equilibrium in the upper ocean before simulating ocean biogeochemistry.

A preindustrial CO_2 (285 μatm) simulation with full biogeochemistry (using MARBL with four PFTs, including coccolithophores) was branched from the ocean physics spinup. Macronutrients and oxygen were initialized from World Ocean Atlas version 2 (Locarnini et al., 2013), while alkalinity and preindustrial dissolved inorganic carbon were initialized from GLobal Ocean Data Analysis Project (GLODAPv2; Lauvset et al., 2016). Other biogeochemical tracers were initialized from previous CESM simulation output; coccolithophore PFT-associated tracers were initialized using small phytoplankton PFT fields. The preindustrial (285 μatm) control simulation was integrated for an additional 150 years (full simulation length is 250 years). Higher CO_2 simulations (at 400, 600, 700, and 900 μatm) were branched off of the preindustrial simulation at year 200, introducing the atmospheric CO_2 increase as a step function change and holding circulation constant. These were integrated for an additional 50 years to achieve equilibrium in upper ocean dissolved inorganic carbon. Comparisons of coccolithophore growth and calcification among different CO_2 levels are conducted for each simulation at the point corresponding to year 250 of the control. We correct for a small drift in the calcium carbonate production (0.001 Pg C/year^{-2} global integral) when analyzing our results.

We quantify coccolithophore responses to increasing CO_2 within marine biomes, as defined by Fay and McKinley (2014). These static biomes were computed from observations and interpolated onto the CESM displaced pole grid. Here we focus our analysis on the subpolar and subtropical seasonally stratified biomes in the North Atlantic, North Pacific, and Southern Ocean.

3. Coccolithophore Model Validation

In this section, we compare properties of the modeled coccolithophore population to those observed in the present-day ocean. Model evaluation is conducted using year 250 output from the simulation run under present-day CO_2 (400 μatm; see above for simulation details). Our validation makes use of satellite-derived PIC (Balch et al., 2005), a large compilation of coccolithophore biomass estimates derived from shipboard measurements (O'Brien et al., 2013), a global compilation of coccolithophore calcification rates (Daniels et al., 2018), and estimates of globally integrated annual upper ocean calcification rates derived from multiple methods. We note that these observations contain substantial uncertainty. For instance, while satellite-derived PIC provides a proxy for coccolithophore abundance, errors can arise from atmospheric correction and inclusion of other suspended minerals (see Balch et al., 2005). We also compare our results to the MAREDAT data set (MARine Ecosystem DATa; Figures 2a–2c; Buitenhuis et al., 2013; O'Brien et al., 2013) and a recent global compilation of coccolithophore calcification rates (Figures 2d–2e; Daniels et al., 2018). The MAREDAT data compilation, based on ~11,000 individual field observations (spanning a time period of 1929 to 2008), derives monthly, depth-specific estimates of total coccolithophore biomass at various points in the ocean. Thus, MAREDAT is subject to considerable uncertainties associated with cell counts, unidentified species, and conversions of cell abundance to biomass (O'Brien et al., 2013). The Daniels et al. calcification data set includes 2765 field calcification measurements spanning a time period from 1991 to 2015. Major gaps in geographical coverage exist in both the Daniels et al. (2018) data set (e.g., western Pacific) and the MAREDAT data set (e.g., Southern Ocean). Furthermore, coccolithophore blooms are spatially variable from year to year (Hopkins et al., 2015), and both of these data sets are highly dependent on when calcification rates were recorded in situ. Despite these uncertainties, the observations presented here comprise the best available metrics for model validation and, taken together, can provide insights on model strengths and weaknesses. We show that, though not perfect, our CESM-cocco achieves reasonable

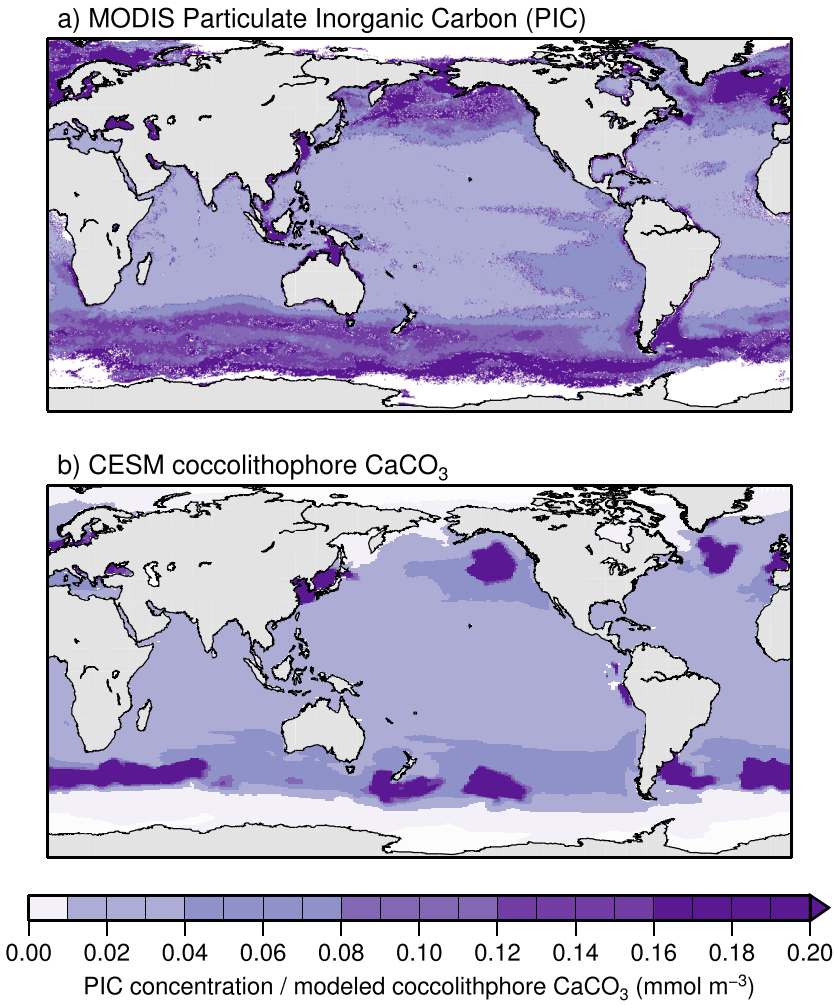

Figure 1. (a) Climatological mean annual particulate inorganic carbon (PIC) derived from Moderate Resolution Imaging Spectroradiometer (MODIS) satellite observations from 2002–2015, and (b) annual mean coccolithophore $CaCO_3$ in the top 50 m from Community Earth System Model (CESM)-cocco.

results with respect to coccolithophore geographical distribution and overall magnitude of coccolithophore calcification and carbon pools.

Figure 1a shows annual mean PIC concentration at 9-km resolution derived from the Moderate Resolution Imaging Spectroradiometer Aqua, averaged over 14 years (2002–2015; Balch et al., 2005). We compare this to the top 50-m average coccolithophore $CaCO_3$ from CESM-cocco (Figure 1b). Low to middle latitudes show low, but ubiquitous coccolithophore PIC; this is captured in our model. Regions of high coccolithophore $CaCO_3$ in the North Atlantic are reasonably captured, but somewhat too far south in our simulations. Though CESM simulates a band of coccolithophore $CaCO_3$ in the Southern Ocean (Great Calcite Belt; Balch et al., 2016), it tends to be particularly concentrated in certain regions (Figure 1b). We speculate this longitudinal heterogeneity is due to an interplay of iron and carbon limitation of the coccolithophore PFT and iron and SiO_3 limitation in the diatom PFT in the CESM Southern Ocean, causing spatial variations in PFT dominance (Figure S3). Similarly, the PIC data suggests a more dispersed coccolithophore presence in the North Pacific. The PIC data also depicts moderate coccolithophore abundance in some eastern boundary upwelling systems (e.g., Peruvian and Benguela upwelling regions), which is not captured in CESM.

We compare the MAREDAT and Daniels et al. (2018) observational data sets to model output during the growing season (June-July-August means in the Northern Hemisphere and December-January-February means in the Southern Hemisphere) at various depth intervals (maps divided into N/S Hemispheres by a black line to separate June-July-August/December-January-February means of data; Figure 2). The MARE-

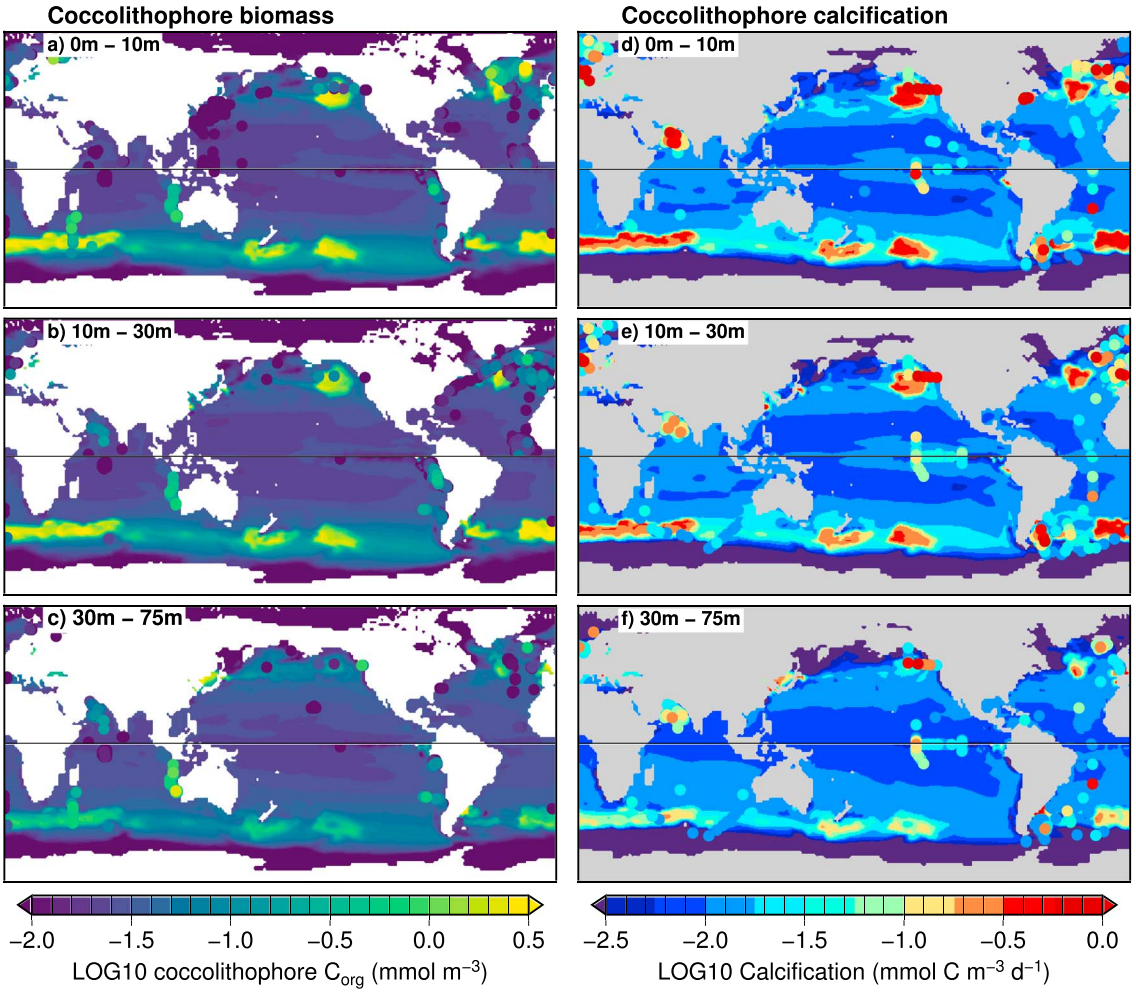

Figure 2. Coccolithophore organic carbon (C_{org}; panels a–c) and coccolithophore calcification (panels d–f) for various depth intervals as simulated by Community Earth System Model-cocco during the growing season (June-July-August mean for Northern Hemisphere and December-January-February mean for Southern Hemisphere; division shown by black line at equator). Dots plotted on top of model output are coccolithophore biomass estimates from growing season means of MARine Ecosystem DATa (O'Brien et al., 2013) for panels (a)–(c), and calcification measurements from Daniels et al. (2018) for panels (e)–(f).

DAT observations are plotted for only the growing season months for each hemisphere, while all the calcification observations are included due to a known growing season bias in the data set (Daniels et al., 2018). In most regions modeled coccolithophore biomass is on the same order of magnitude as shown in MAREDAT. However, like the PIC data, coccolithophores in the model are more concentrated in certain regions than the data suggests (e.g., the eastern North Pacific, North Atlantic). MAREDAT estimates tend to be somewhat lower in the tropics and subtropics than depicted in output from CESM with coccolithophores (e.g., see Figure 2a in the western Pacific). The model agrees best with the MAREDAT data in the Atlantic ocean, but blooms in the North Atlantic tend to be further north than captured in our model (Figure 2). Unfortunately, there are sparse MAREDAT coccolithophore biomass estimates in the Southern Ocean with which to compare our model results, but a transect in the Indian sector of the Southern Ocean shows reasonable agreement in the surface ocean (Figure 2a). CESM-cocco underestimates coccolithophore biomass in the deeper waters of the northern Indian Ocean and in the southeastern parts of the Indian and Pacific oceans (Figure 2b).

The calcification rate comparison shown in Figures 2d–2f shows that geographical patterns of calcification are captured by CESM-cocco for important coccolithophore regions such as the North Atlantic, Patagonian shelf region, and the North Pacific. Calcification in some parts of the calcite belt in the Southern Ocean are overestimated in the model according to the available data (Figures 2e and 2f). The most obvious model underestimations with regard to calcification are in the equatorial eastern Pacific and the northern Indian

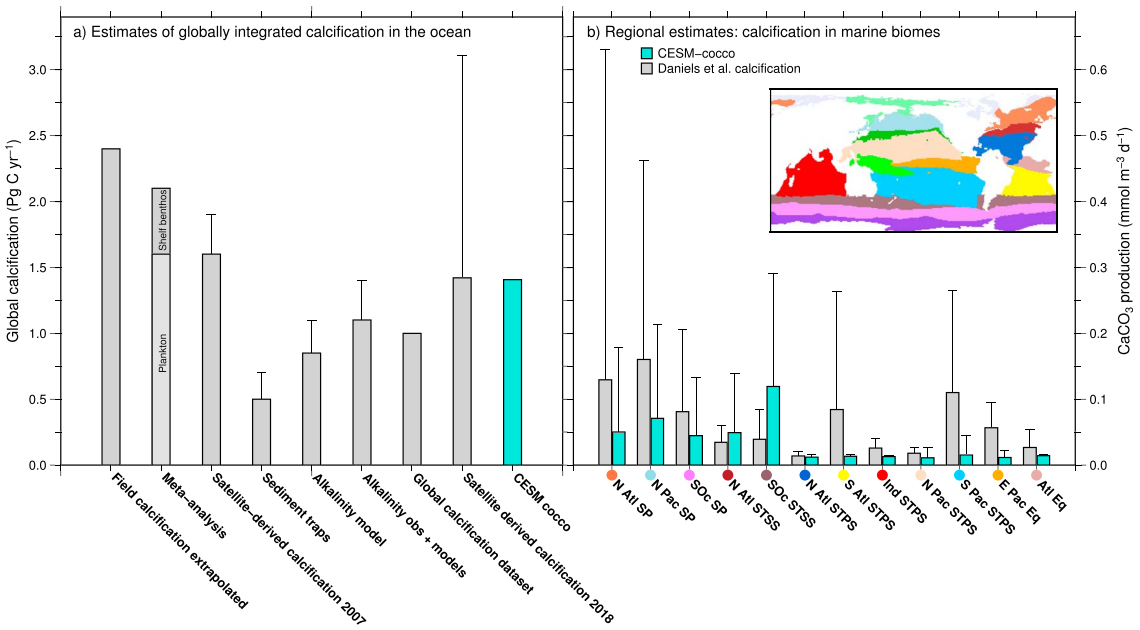

Figure 3. An observation-model comparison of upper ocean calcification. (a) Observation-based estimates of global $CaCO_3$ production in the upper ocean (gray) and globally integrated $CaCO_3$ production in the top 150 m from CESM-cocco (turquoise). All values are in units of Pg C/year. References for observation-based estimates are as follows: field calcification extrapolated (Marañón et al., 2016), Meta-analysis (Smith & Mackenzie, 2016), satellite-derived calcification 2007 (Balch et al., 2007), sediment traps (Iglesias-Rodriguez et al., 2002; Milliman et al., 1999), alkalinity model (Sarmiento et al., 2002; Lee, 2001), alkalinity observations, and modeling (Feely et al., 2004), global calcification data set (Daniels et al., 2018), and new satellite derived calcification (Hopkins & Balch, 2018). (b) Mean calcification in the surface ocean (0–10 m) for various marine biomes (shown on map, with colors corresponding to colored dots next to biome names; Fay & McKinley, 2014); observations from Hopkins and Balch (2018; gray) are compared to CESM-cocco calcification (turquoise). Error bars in panel (a) refer to the total range if multiple studies are cited or error reported in a specific study if only one reference is cited. Error bars in panel (b) depict standard deviation in spatial averaging within biomes; there were at least two calcification measurements in each biome shown along the *x* axis (biomes with less than five data points are not shown). CESM = Community Earth System Model.

Ocean. Though the MAREDAT data show slightly higher coccolithophore biomass in the Indian Ocean than the model (>10-m depth; Figures 2b and 2c), satellite-derived PIC concentration is low in this region (Figure 1). Unlike the calcification data set, PIC and MAREDAT data both suggest low coccolithophore abundance in the equatorial Pacific (Figures 1 and 2). Thus, the evaluation of the model in these regions depends on which observations are compared to the model.

Another important metric to capture in our model is total globally integrated annual $CaCO_3$ production in the upper ocean, as this can strongly influence the alkalinity pump. We compiled various estimates of total annual upper ocean calcification derived using a variety of methods and compare this to results from CESM-cocco (Figure 3a). While coccolithophores perform a substantial portion of upper ocean calcification, other organisms such as foraminifera, also contribute to calcification observations in the real ocean. In CESM-cocco the coccolithophore PFT is the only source of $CaCO_3$ in the upper ocean. Observation-based calcification estimates span an order of magnitude, ranging from 0.5 to 2.4 Pg C in $CaCO_3$ per year (Figure 3a; Balch et al., 2007; Daniels et al., 2018; Feely et al., 2004; Hopkins & Balch, 2018; Iglesias-Rodriguez et al., 2002; Lee, 2001; Marañón et al., 2016; Milliman, 1993; Sarmiento et al., 2002; Smith & Mackenzie, 2016). CESM-cocco estimates global upper ocean (top 150 m) calcification at present-day CO_2 concentration to be ~1.4 Pg C/year, falling squarely within this range (see turquoise bar in Figure 3) and coinciding well with a recent satellite derived estimate of 1.42 Pg C/year by Hopkins and Balch (2018). While some of these observation-based estimates include all marine calcifiers (e.g., Milliman, 1993; Sarmiento et al., 2002; Smith & Mackenzie, 2016), others quantify coccolithophore calcification explicitly (e.g., Balch et al., 2007; Hopkins & Balch, 2018).

Figure 3b shows a regional comparison of calcification rates within marine biomes (Fay & McKinley, 2014) using surface calcification rates from Daniels et al. (2018). While standard deviations (calculated from spatial within-biome variation for the model, shown by error bars) overlap between the model and data for all regions, observational calcification estimates in the subpolar biomes of the North Pacific, North Atlantic,

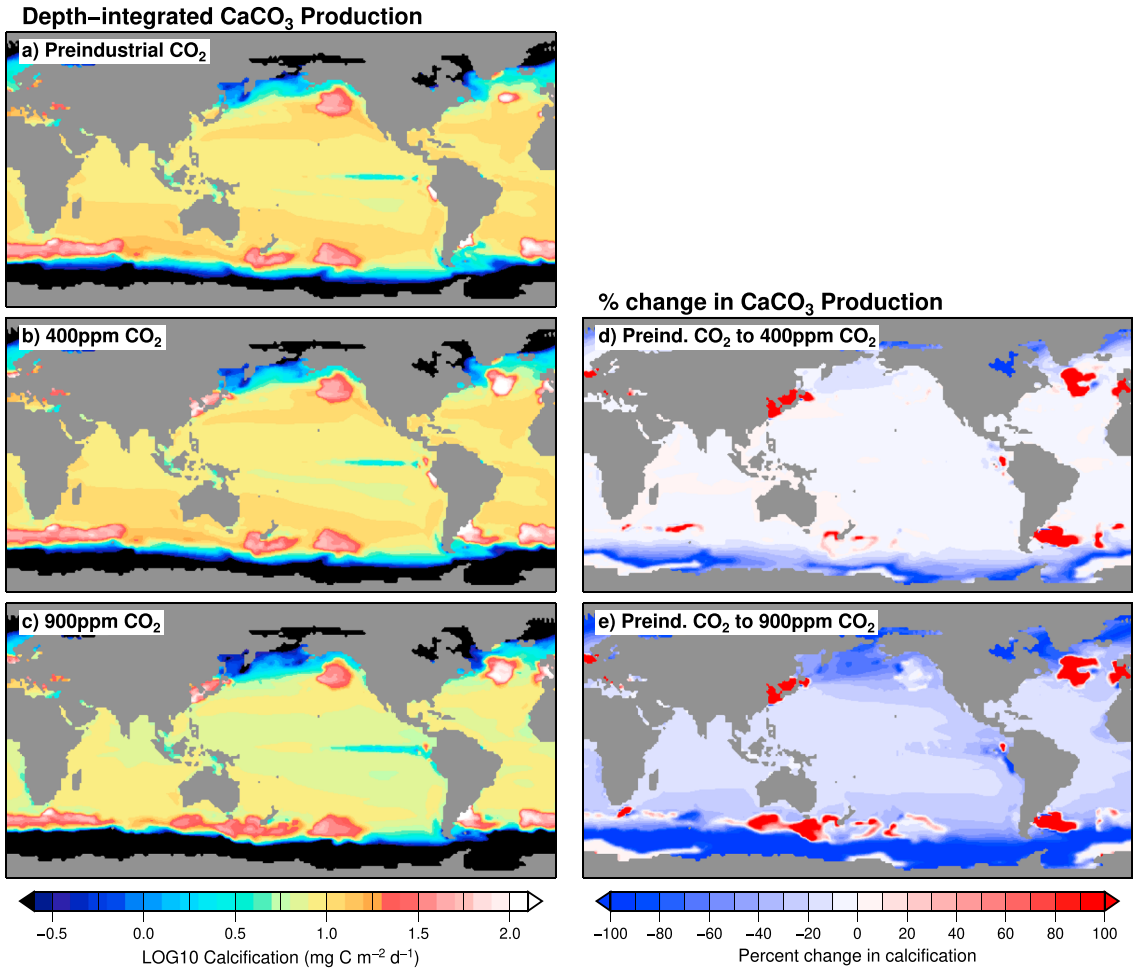

Figure 4. Depth integrated $CaCO_3$ production by coccolithophores under varying CO_2 levels: (a) preindustrial (285 μatm), (b) modern (400 μatm), and end-of-the-century high-concentration scenario (900 μatm). Percent change in depth integrated calcification from preindustrial CO_2 to 400 and 900 μatm are presented in panels (d) and (e), respectively.

and Southern Ocean are higher than the model. However, calcification in the subtropical seasonally stratified biomes in the North Atlantic and Southern Ocean is larger in the model than in the observations, suggesting that CESM-cocco coccolithophore blooms occur slightly equatorward of their observed positions (there is no calcification data in the subtropical seasonally stratified biome in the North Pacific with which to compare). The subtropical permanently stratified biomes show slightly higher calcification rates in the observations than depicted in the model, though the large error bars associated with the calcification observations indicate high spatial variability in these biomes (STPS biomes in Figure 3).

In general, CESM-cocco captures important observed geographical coccolithophore characteristics (e.g., the North Atlantic summertime bloom, Southern Ocean calcite belt, seasonal presence in the North Pacific, and ubiquitous low biomass at low latitudes). In the following sections we analyze results from simulations testing the effects of anthropogenic CO_2 increases on coccolithophores.

4. Results and Discussion

4.1. The Sensitivity of $CaCO_3$ Production to Increasing CO_2

From preindustrial to modern day CO_2 concentrations, the model simulates both decreased and increased calcification depending on the geographical region (Figures 4 and S4). It is important to note that calcification changes in CESM-cocco depend on two quantities: coccolithophore organic C-specific growth rate and the coccolithophore $r_{CaCO_3:C}$ ratio, used to convert organic C-specific growth rates to calcification. Coccolithophore calcification decreases slightly in most regions of the ocean as coccolithophore $r_{CaCO_3:C}$ decreases

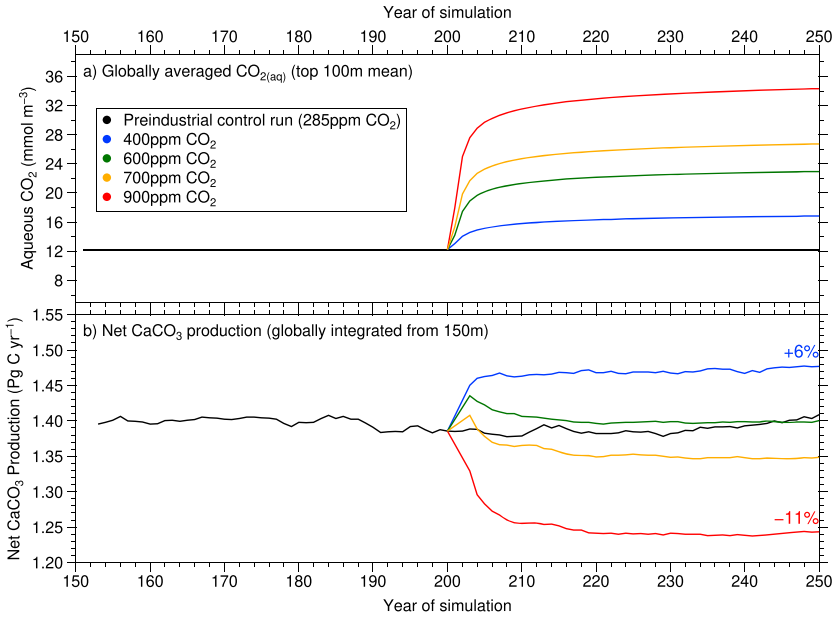

Figure 5. Top 100-m mean $CO_{2(aq)}$ (a) and net depth-integrated $CaCO_3$ production (b) versus year of simulation for the Community Earth System Model simulations used in this study with preindustrial CO_2 (black), 400 μatm CO_2 (blue), 600 μatm CO_2 (green), 700 μatm CO_2 (orange), and 900 μatm CO_2 (red). Time series of $CaCO_3$ production are drift-corrected (by subtracting a 0.001 Pg C/year^{-2} drift from the global integral) and filtered by a 5 year running mean. Indicated percent changes for the 400 and 900 μatm CO_2 are relative to the preindustrial simulation.

from rising CO_2 (by 0.2 to 1 mg C·m^{-2}·day^{-1}, a 1–10% decrease; light blue areas in Figure 4d). However, certain regions such as in the North Atlantic, Patagonian Shelf, and western Pacific show stark increases in depth-integrated calcification at 400 μatm relative to preindustrial CO_2 levels (>90% increase; red areas in Figures 4d and S4). As coccolithophore $r_{CaCO_3:\dot{r}C}$ decreases under increased CO_2 (equation (2)), the only way to achieve increased calcification under increasing CO_2 is for there to be more coccolithophores. In these regions, coccolithophores, stimulated by the additional carbon in the water column, increase their growth rate (see Figure S5 for changes in coccolithophore growth rate from increasing CO_2) and compete with other PFTs more effectively for resources, thus increasing their abundance and overall calcification in these parts of the ocean. These increases in calcification from preindustrial to modern day CO_2 concentrations outweigh the decreases in other regions, resulting in a 6% global increase relative to preindustrial CO_2 levels (Figure 5 and Table 2).

A similar geographic pattern emerges when comparing preindustrial calcification with that under high CO_2 (900 μatm; Figure 4e), but with a different response on a global scale. With an atmospheric CO_2 concentration of 900 μatm, the effect of OA on calcification is much stronger than under modern CO_2. Therefore the model shows ~20% declines in $CaCO_3$ production in the tropics and subtropics with 90–100% declines at high latitudes (1.2 to >2 mg C in $CaCO_3$·m^{-2}·day^{-1} declines; see Figures 4e and S4). We still observe some regional increases in modeled calcification, as in the modern CO_2 experiment (Figure 4d), but in

Table 2
Globally Integrated $CaCO_3$ Production in the Upper 150 m from CESM With Coccolithophore Under Various CO_2 Levels, With Percent Change From Preindustrial and Present-Day CO_2 Conditions

Representative time period	CO_2 (μatm)	Global $CaCO_3$ production (Pg C/year)	% change from preindustrial	% change from present
Preindustrial	285	1.41	—	—
Modern	400	1.49	+6%	—
Future	600	1.40	−0.2%	−6%
Future	700	1.35	−4%	−9%
Future	900	1.24	−11%	−17%

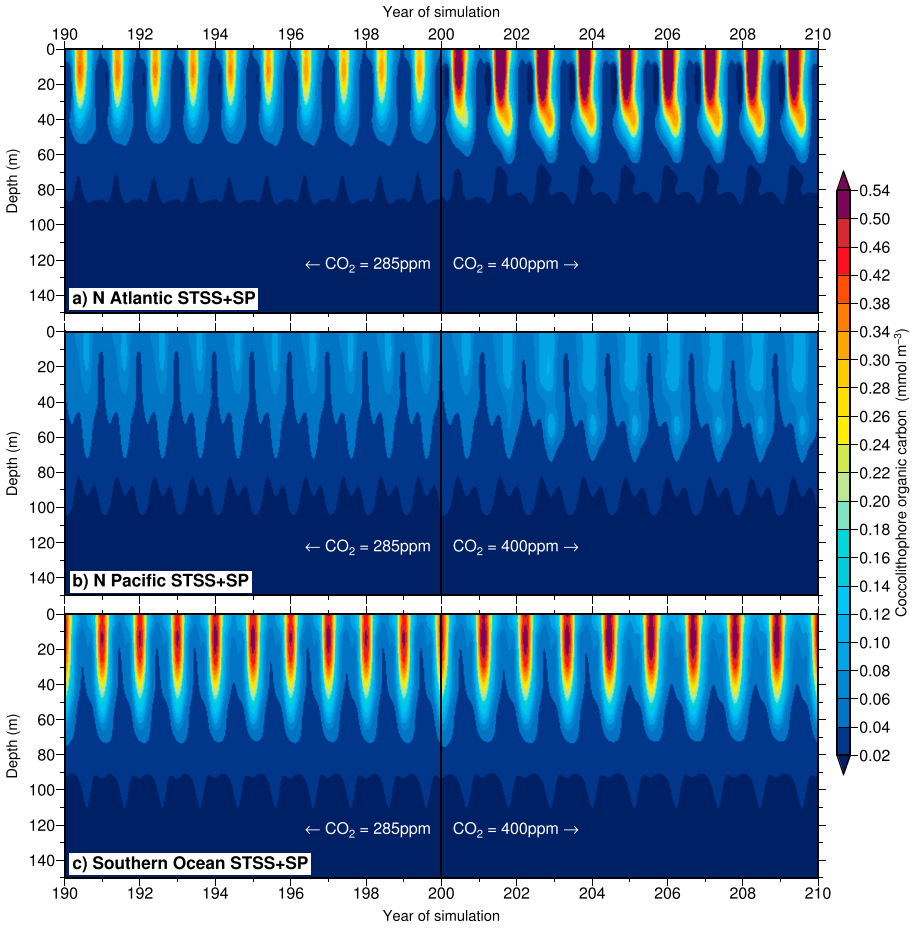

Figure 6. Time-depth coccolithophore organic carbon (C_{org}) averaged over the area covered by subtropical seasonally stratified (STSS) and subpolar (SP) biomes (Fay & McKinley, 2014) in the (a) North Atlantic, (b) North Pacific, and (c) Southern Ocean. The last 10 years the preindustrial control simulation are followed by the first 10 years of the modern (400 μatm CO_2) simulation (division indicated by black vertical line).

this high-CO_2 case, the widespread declines in calcification from OA outweigh these increases on a global scale. Thus, relative to preindustrial calcification, the model shows a decline in global calcification by 11% in this high-CO_2 world (Figure 5b and Table 2) relative to preindustrial (or −17% relative to modern). Two midcentury CO_2 level experiments (600 and 700 μatm; green and orange lines on Figure 5b) indicate that the compensation point between the OA effect and the carbon fertilization effect on globally integrated calcification occurs at roughly 600 μatm atmospheric CO_2.

4.2. Regional Changes in Coccolithophore Abundance Within the Phytoplankton Community

As described in the previous section, from preindustrial CO_2 levels to present-day CO_2, coccolithophores increase in abundance in certain parts of the ocean. We observe the largest increases in coccolithophore calcification near the boundary of the subtropical and subpolar gyres in the North Atlantic, North Pacific, and Southern Oceans (Figure 4d). We chose to focus on changes occurring in subtropical seasonally stratified and subpolar biomes of the North Atlantic, North Pacific, and Southern Ocean because these are major coccolithophore regions in today's oceans and CO_2 stimulated increases in coccolithophore carbon in the model tend to occur in these two biomes. In Figure 6 we quantify coccolithophore organic C biomass in a depth versus time field. This figure shows the last 10 years of the preindustrial simulation followed by the first 10 years of the modern (400 μatm) CO_2 simulation in these two biomes in these three regions (see maps on Figure 7 for region boundaries). Coccolithophores expand in the upper ocean in each region, albeit with unique depth patterns. In the North Atlantic, we observe an increase in peak coccolithophore biomass from 0.6 to 1 mmol/m^3 and a deepening of coccolithophores from ~40 to 55 m with a lengthened growing season (by 1 month, growing season defined as when coccolithophore carbon concentration >0.2 mmol/m^3).

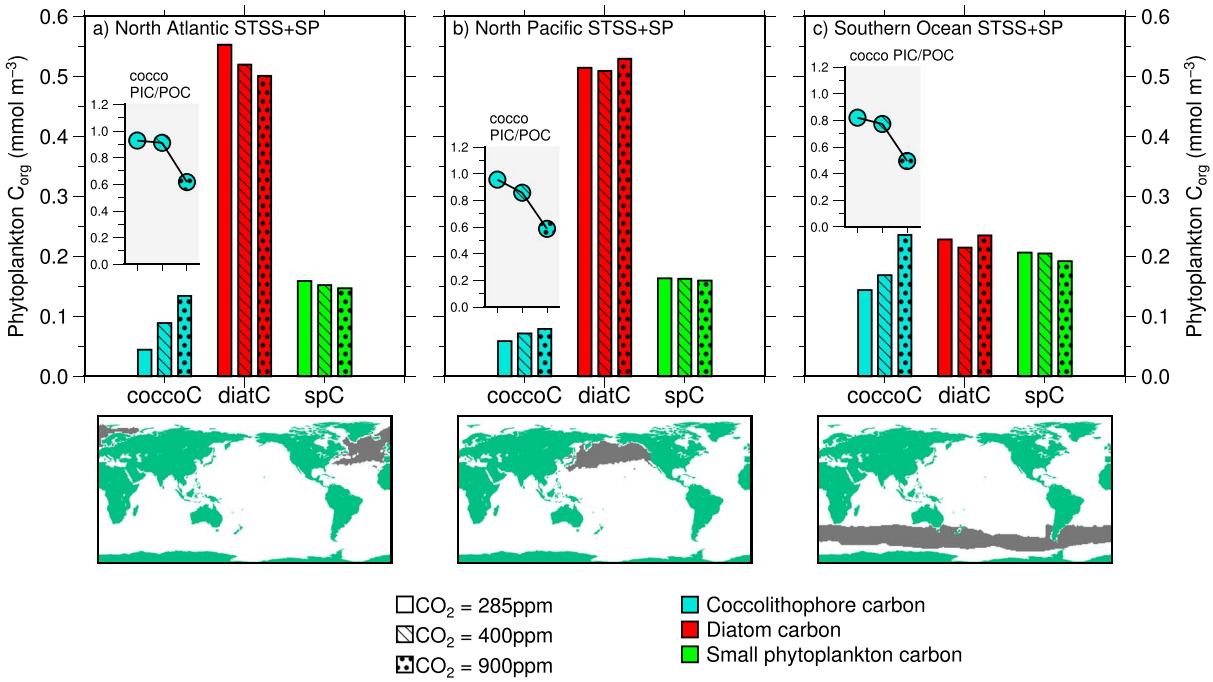

Figure 7. Top 100-m mean phytoplankton organic carbon (C_{org}) in the subpolar and subtropical seasonally stratified biomes in the (a) North Atlantic (June-July-August-September mean), (b) North Pacific (June-July-August-September mean), and the (c) Southern Ocean (December-January-February mean) for the final year of each simulation (year 250). Simulations with preindustrial CO_2 (285 μatm) are solid bars; modern CO_2 (400 μatm) shown by hatched bars; end-of-the-century (900 μatm) shown by dotted bars. Diazotroph carbon is not included due to their minor contributions to phytoplankton biomass in these biomes. Particulate inorganic carbon to particulate organic carbon (PIC/POC) ratios in coccolithophore biomass are plotted above the coccolithophore carbon bars. Maps along the bottom of the figure show the region over which mean carbon pools are averaged. STSS = subtropical seasonally stratified; SP = subpolar.

We note that the seasonal cycle of present-day North Atlantic coccolithophore abundance in CESM-cocco aligns well with the two seasonally resolved observations of coccolithophore abundance proxies (Figure S6). In the North Pacific, coccolithophores increase slightly in abundance at the surface and in the deep chlorophyll maximum (~50 m deep) after being exposed to 400 μatm CO_2. Finally, in the Southern Ocean we observe a small mean increase in the organic carbon pool associated with coccolithophores (e.g., at the surface coccolithophore carbon increases from 0.6 to 0.7 mmol/m^3 during January, the peak of the bloom; Figure 6c).

The alleviation of carbon limitation can only have a pronounced effect on coccolithophore biomass if all other growth resources are relatively plentiful. Therefore, it is sensible that in the North Pacific we see an expansion of coccolithophore carbon in the deep chlorophyll maximum, where nutrients and light are both moderately abundant. This is also why we see a pronounced effect of carbon fertilization on coccolithophores in the intergyre regions (where subpolar and subtropical gyres meet; red areas in the North Atlantic and Southern Ocean in Figures 4d and 4e); here, there is sufficient light and nutrients to support additional coccolithophore growth with more CO_2 availability.

Regions of coccolithophore increases are marked by changes in the phytoplankton community, suggestive of a potential shift in the ecological assemblage that could occur under ever increasing CO_2. In the North Atlantic, coccolithophores increase in abundance from low to high CO_2, mainly at the expense of diatoms (Figure 7a). The North Pacific also shows only slight rearrangements of phytoplankton communities, with diatoms increasing slightly under 400 μatm CO_2, and no significant change in small phytoplankton abundance. In our modeled Southern Ocean, coccolithophores increase substantially with increasing CO_2 (Figure 7c), but diatoms and small phytoplankton groups do not systematically decline by a similar extent. The phytoplankton carbon pools indicated in Figure 7 are averaged geographically over a large region (see maps along the bottom of the figure), as well as over the top 100 m; shifts in phytoplankton community structure are clearer if examining only areas where increases in coccolithophore abundance has occurred (i.e., the red areas on Figures 4d and 4e). For instance, we observe ~90% decline in mean top 100-m diatom biomass in the North Atlantic where marked coccolithophore increases occur from preindustrial CO_2 to 900

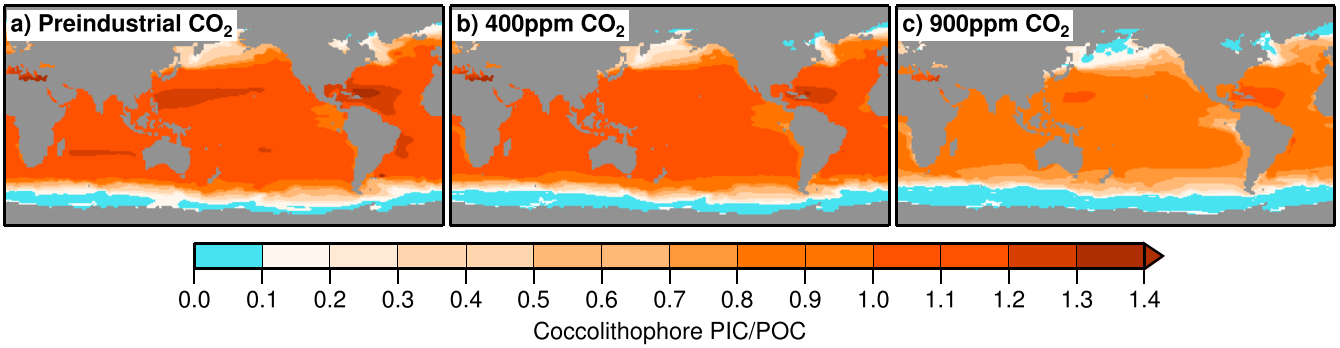

Figure 8. Coccolithophore particulate inorganic carbon/particulate organic carbon (PIC/POC) ratio under (a) preindustrial CO_2, (b) 400 μatm, and (c) 900 μatm.

μatm CO_2. Further, over this same CO_2 change, diatoms on the Patagonian shelf decrease by ~20%, while coccolithophores show a ~100% increase (not shown). These types of dramatic shifts in phytoplankton dominance, however, can be due to the simplified ecosystem in CESM (i.e., only one grazer) and may simply suggest the direction of an ecological shift.

The changes in coccolithophore abundance and calcification from preindustrial CO_2 to modern CO_2 levels in certain regions of the ocean are supported by recent observations and modeling results. Increases in coccolithophore abundance over the last several decades has been reported in the subtropical and subpolar North Atlantic (Krumhardt et al., 2016; Rivero-Calle et al., 2015). Both of these studies indicated carbon fertilization as the primary cause for this increase. Furthermore, a decrease in the opal:carbonate ratio in sediment traps in the Sargasso Sea and at 48°N in the North Atlantic since the 1980s (Antia et al., 2001) indicates the coccolithophore expansion may be at the expense of diatoms, as shown here (Figure 7a). In support of these results, Furukawa et al. (2018) used a model based on cellular physiology to show that coccolithophores will likely increase in abundance (as diatoms decrease) as CO_2 increases, particularly in oligotrophic regions. Additionally, a poleward expansion of coccolithophores in all ocean basins was shown using historical satellite data and a compilation of in situ samples spanning >60 years, citing increasing CO_2 and temperature as likely reasons for the increase (Winter et al., 2013). Further, a recent study from the Southern Ocean reports decreases in calcification over the satellite record (Freeman & Lovenduski, 2015). This is supported by our model, as total calcification for the Southern Ocean subpolar biome decreases as CO_2 increases (data not shown). Indeed, as the organic carbon pool associated with the coccolithophore PFT increases, relative coccolithophore $CaCO_3$ generally decreases with increasing CO_2 (see inset "cocco PIC/POC" plots on Figure 7).

Our study suggests that while coccolithophores expand with increasing CO_2 availability, they become more lightly calcified. In the North Pacific, Southern Ocean, and far North Atlantic, regions with coccolithophore PIC/POC biomass ratios <0.1 expand under 900 μatm CO_2 (light blue areas of Figure 8), indicating that $CaCO_3$ formation is approaching zero under such high CO_2 levels. This is indicative of conditions that may favor "naked" coccolithophores (i.e., coccolithophores without $CaCO_3$ shells), as has been observed in laboratory experiments with the Southern Ocean morphotype of *Emiliania huxleyi* at high CO_2 levels (~1,200 μatm; Müller et al., 2015). It is important to note that our parameterization does not include possible detrimental effects of high CO_2 on growth rate (see section 4.4 below). Greatly reduced calcification by coccolithophores under high CO_2 levels and increased temperature was also observed in community incubation experiments from the North Atlantic (Feng et al., 2009). According to our simulations, coccolithophores with almost no PIC component to their biomass could be present in some regions of the Southern Ocean even at today's CO_2 concentrations (Figure 8b); these areas, however, are generally too cold for coccolithophore growth. Though naked coccolithophore cells have not been observed in natural populations, they could be easily overlooked since differentiating them from other spherical nanoplankton would be nearly impossible (Müller et al., 2015). In any case, coccolithophores in some subpolar regions could be nearly without a $CaCO_3$ coccosphere by the end of the century according to these simulations. Whether reduced calcification could affect their survival is still an open question (Monteiro et al., 2016). Oceanic environments that show greatly reduced $CaCO_3$ formation could, however, have important effects on regional and global biogeochemistry.

4.3. Implications for Biogeochemistry

The changes in coccolithophore growth and calcification under increasing CO_2 described here could have consequences for ocean biogeochemistry. Overall, as CO_2 concentrations in the atmosphere continue to increase, we can expect more coccolithophores, but with less calcified exteriors. Through the formation of their $CaCO_3$ shells, marine calcifiers remove alkalinity from the ocean surface (increasing pCO_2), while ballasting organic carbon to depth (following the hypothesis that ballast minerals determine deep water POC fluxes; Armstrong et al., 2002). Furthermore, changes in diatoms (Figure 7a), which produce an opal shell, could also impact carbon export. Therefore, changes in shell formation could affect the export ratio of photosynthetically derived organic matter relative to primary production from the photic zone (the export ratio, i.e.,"e-ratio"), as well as air-sea flux of CO_2, two important processes in the oceanic carbon cycle.

As coccolithophores calcify less under increasing CO_2, sinking particulates containing coccolithophores cells, fecal pellets of zooplankton having consumed coccolithophores, and other marine aggregates could become less dense. These processes are parameterized in CESM with a mineral ballast model with possible implications for the e-ratio (Armstrong et al., 2002). The potential for remineralization before reaching the sea floor is increased with less ballast minerals (see section 2 for a summary of the ballast model). Indeed, an analysis of CO_2-induced changes in the e-ratio at 100 m of depth (total POC exported at 100 m divided by net primary production) between simulations at preindustrial CO_2 versus 900 μatm CO_2, indicate that most areas of the ocean show slight decreases in the e-ratio under future CO_2 conditions (see Figure S7 for a map of e-ratio changes). However, regions where the carbon fertilization effect on coccolithophores is dominant show large increases in the e-ratio, balancing the widespread decreases. As such, there is no significant change to the global average e-ratio from preindustrial to 900 μatm CO_2 according to these simulations. However, regional effects could be more pronounced (e.g., e-ratio increases in the North Atlantic and decreases in the Southern Ocean). It is important to note, however, that CO_2-induced climatic warming and accompanying stratification (which are not included here) could affect these e-ratio changes through alterations to marine primary production (Fu et al., 2016; Krumhardt et al., 2017b; Kvale et al., 2015b).

Less calcified coccolithophores in the future also mean decreased removal of alkalinity from the surface ocean. This has the potential to affect the overall amount of CO_2 that the ocean absorbs from the atmosphere. While our model configuration does not allow us to explore this question directly, we performed a back of the envelope calculation to evaluate how changes in alkalinity resulting from decreased calcification could affect air-sea CO_2 gas exchange. We calculated the difference in potential alkalinity from year 250 of the 900 μatm CO_2 simulation relative to preindustrial CO_2 simulation; this represents the change in alkalinity due solely to changes in calcification (Sarmiento & Gruber, 2006). We subsequently converted this change in potential alkalinity (from preindustrial to 900 μatm CO_2) to a change in CO_2 flux using established procedures (e.g., Lovenduski et al., 2007). While some regions show decreased CO_2 fluxing into the ocean (areas where coccolithophore abundance, and thus overall calcification, is greater under increased CO_2), most areas of the ocean show increased CO_2 flux into the ocean from decreasing calcification under increased CO_2. This results in an ~2 Pg/year increase in oceanic absorption of CO_2 at 900-μatm atmospheric CO_2, a negative feedback on increasing anthropogenic atmospheric CO_2. This is in line with previous model studies that found a negative feedback on rising CO_2 concentration through a reduction in pelagic calcification (Gangstø et al., 2011; Gehlen et al., 2007; Pinsonneault et al., 2012; Ridgwell et al., 2007).

4.4. Limits of This Study

While we isolate the effects of CO_2 on coccolithophores in this study, other simultaneous effects of climate change could exert a confounding influence on both the C-specific growth rate of coccolithophores, as well as their calcification. As described in Krumhardt et al. (2017a), increasing temperatures in high latitude regions may offset some of the OA effects on coccolithophore calcification (see also Kvale et al., 2015b). In addition, warming-induced ocean stratification could decrease available nutrients and slow coccolithophore photosynthesis (contrasting with the carbon fertilization effect described in this study). Increased nutrient limitation could also increase coccolithophore $r_{CaCO_3:C}$ (Krumhardt et al., 2017a). However, increasing temperatures in tropical regions could cause decreased tolerance to acidic conditions, as shown by the exclusion of extracellular coccolithophore calcifiers during the Paleocene-Eocene Thermal Maximum in low latitude regions (Gibbs et al., 2016). These additional effects of climate change could modulate some of the results shown here.

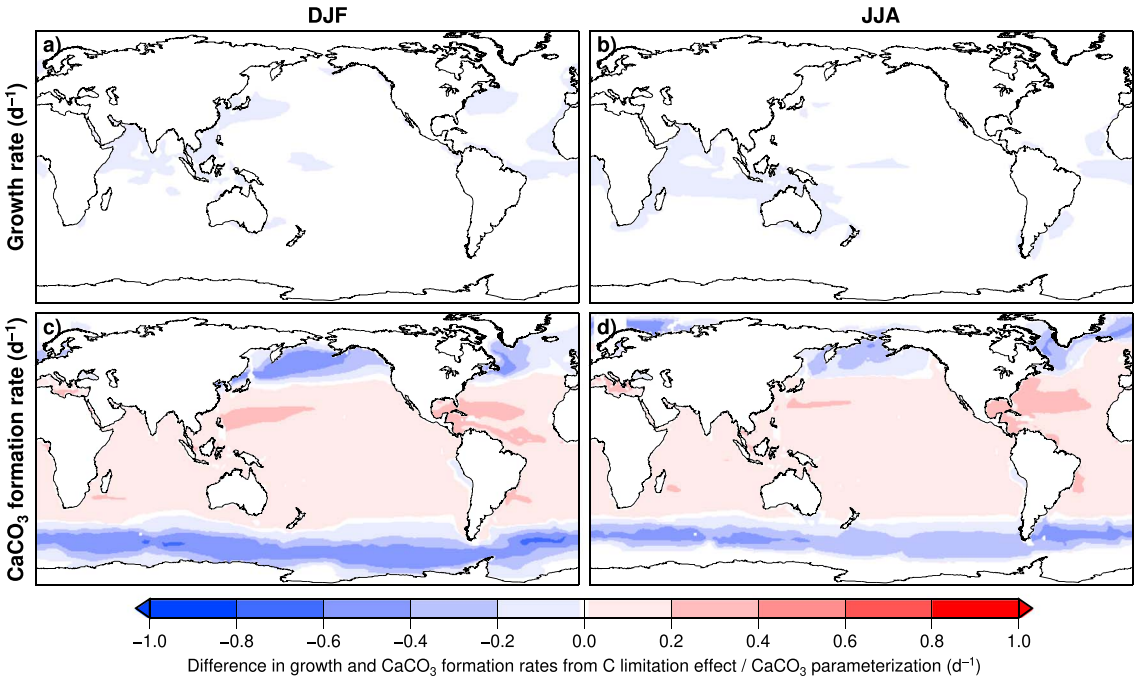

Figure 9. Testing the effect of carbon sensitivity on coccolithophore growth and calcification at the ocean surface. Panels (a) and (b) show the change in coccolithophore growth rate (day^{-1}) that occurs from adding carbon limitation of coccolithophores to the model during December-January-February (DJF; panel a) and June-July-August (JJA; panel b). Panels (c) and (d) show the change in $CaCO_3$ formation rate that occurs due to variations in $r_{CaCO_3:C}$ employed in CESM-cocco (sensitive to $CO_{2(aq)}$, PO_4 limitation, and temperature; see section 2) as opposed to uniformly applying a mean coccolithophore $r_{CaCO_3:C}$ ratio of 1 (Krumhardt et al., 2017a). This sensitivity test was conducted "offline" using output (sea surface temperature, $CO_{2(aq)}$, limitation terms for nutrients, and light) from year 250 of the 400-μatm simulation, thus providing a mean state sensitivity assessment for approximate magnitudes of these rates.

As in any modeling study, there are uncertainties inherent in representing the real world in a simplified way. Not only is the physical ocean model subject to model bias, but here we simulate four PFTs and one zooplankton, a vast underrepresentation of true marine planktonic biodiversity. For instance, coccolithophores are not the only major calcifiers in the pelagic ocean. Major zooplankton calcifiers, such as planktonic foraminifera and pteropods, are not represented in this version CESM. Though increasing CO_2 has been shown to have similar negative effects on zooplankton calcification as shown for coccolithophores (Davis et al., 2017; Moy et al., 2009; Orr et al., 2005), a separate aragonite producer zooplankton class (e.g,. pteropods) may be necessary to simulate the full effects of OA on marine calcifiers (Gangstø et al., 2008). Even within the coccolithophore PFT, biodiversity may be underrepresented; our parameterization is based on coccolithophore species with which physiological experiments have been performed, most of which are Northern Hemisphere isolates (Krumhardt et al., 2017a). Subtropical coccolithophores, such as those of the genus *Umbellosphaera* are important components of the coccolithophore community in the subtropics and have not been included here due to lack of physiological testing (Krumhardt et al., 2017a; Poulton et al., 2017).

Indeed, different coccolithophores may respond differently to environmental perturbations, such as increasing CO_2. We aimed to be conservative with respect to coccolithophore carbon limitation by prescribing a low half saturation constant for CO_2 (see section 2) to parameterize the photosynthetic sensitivity to increasing CO_2. However, this may be an oversimplification, as some coccolithophores may not experience carbon limitation and/or unstudied species could respond to increasing CO_2 in unanticipated ways. Therefore, we performed a sensitivity test to explore how the CO_2 sensitivity of the coccolithophore PFT affects growth rates and $CaCO_3$ formation rates (Figure 9). We calculated coccolithophore PFT growth rates in CESM-cocco with and without carbon limitation and calcification rates with and without a variable coccolithophore $r_{CaCO_3:C}$ ratio. Growth rates are slightly decreased due to carbon limitation in some regions (see light blue areas on Figures 9a and 9b). The CESM-cocco parameterization for a variable coccolithophore $r_{CaCO_3:C}$ ratio (sensitive to $CO_{2(aq)}$, PO_4 limitation, and temperature; see section 2) causes $CaCO_3$ formation rates to decrease at high latitudes and increase in low- and middle-latitude regions (Figures 9c and 9d). While this is study is limited to CO_2 concentrations ranging from 285 and 900 μatm, coccolithophore

responses to larger variations in CO_2 and/or during different periods of Earth's history may not be feasible with CESM-cocco. For instance, over long geological timescales, high-CO_2 conditions during the Eocene favored larger coccolithophores with smaller species becoming more common as atmospheric CO_2 declined (Hannisdal et al., 2012; Henderiks & Rickaby, 2007). In agreement, Bolton et al. (2016) showed that allocation of bicarbonate ions between calcification and photosynthesis occurred at different thresholds in large versus small coccolithophores during the Miocene. Thus, longer time scales (2 to 50 million years ago) complicate the $r_{CaCO_3:C}$-CO_2 relationship due to evolutionary selection of smaller coccolithophore species and possible changes in weathering and ocean alkalinity (Bolton et al., 2016; Hannisdal et al., 2012). Increased H^+ ion concentrations could increase the physiological cost of calcification if coccolithophores are unable to adapt (Bach et al., 2015). As discussed above, reduced calcification by coccolithophores in CESM-cocco is not accompanied by decreased fitness (such as increased grazing rates) or reduced competitiveness (Bach et al., 2015), which may not be realistic. Some studies have shown reduced growth rates under CO_2 levels >800 μatm (e.g., Müller et al., 2015), while others do not (e.g., Rost et al., 2003). Furthermore, in CESM-cocco CO_2 only influences coccolithophore growth and calcification, but other phytoplankton groups could also be impacted by increasing $CO_{2(aq)}$ (Dutkiewicz et al., 2015). Finally, being organisms with a fast life cycle and constant environmental pressure, phytoplankton may have the ability to evolve and adapt quickly in the face of global change (Lohbeck et al., 2012), a process which is not modeled here.

5. Conclusions

In this study, we described a novel explicit parameterization of a PFT representative of coccolithophores in the marine ecosystem model in CESM. This PFT is sensitive in both growth rate and calcification to aqueous CO_2 in the water. We use this model to evaluate the sensitivity of coccolithophore growth and calcification to increasing CO_2 both regionally and on a global scale. We show that increasing CO_2 stimulates the growth of coccolithophores in some regions (North Atlantic, Western Pacific, and parts of the Southern Ocean), allowing them to better compete for resources with other PFTs in the model. As CO_2 increases in the upper ocean, however, calcification is impaired. Most regions of the ocean show vast declines in pelagic calcification, with some regions (Southern Ocean and North Pacific) being subject to almost no calcification by coccolithophores at end-of-the-century CO_2 levels. Though CO_2 stimulates growth in some areas, coccolithophores in general are projected to be more lightly calcified under future, high CO_2 conditions. As other effects of climate change may modulate some of the changes showed here, the next step of this research is to perform transient simulations with CESM-cocco under projected climate change scenarios.

Acknowledgments
Source code and instructions for configuring simulations for CESM-cocco can be found at www.doi.org/10.5281/zenodo.2538148 website. Model output from the simulations analyzed here can be found at https://doi.org/10.5065/pkp3‐gv40 website. We would like to thank CISL at the National Center for Atmospheric Research for CESM computing resources used for the simulations in this study. Funding for this research was provided by NSF (OCE-1558225, PLR-1543457, and OCE-1258995). This material is based upon work supported by the National Center for Atmospheric Research, which is a major facility sponsored by the National Science Foundation under Cooperative Agreement 1852977. C. N. was supported by the Swiss Federal Institute of Technology Zürich (ETH Zürich) and the Swiss National Science Foundation (project SOGate, grant 200021_153452).

References

Antia, A. N., Koeve, W., Fischer, G., Blanz, T., Schulz-Bull, D., Schölten, J., et al. (2001). Basin-wide particulate carbon flux in the Atlantic Ocean: Regional export patterns and potential for atmospheric CO_2 sequestration. *Global Biogeochemical Cycles*, *15*(4), 845–862. https://doi.org/10.1029/2000GB001376

Armstrong, R. A., Lee, C., Hedges, J. I., Honjo, S., & Wakeham, S. G. (2002). A new, mechanistic model for organic carbon fluxes in the ocean based on the quantitative association of POC with ballast minerals. *Deep Sea Research Part II: Topical Studies in Oceanography*, *49*(1), 219–236. https://doi.org/10.1016/S0967-0645(01)00101-1, the US JGOFS Synthesis and Modeling Project: Phase 1.

Bach, L. T. (2015). Reconsidering the role of carbonate ion concentration in calcification by marine organisms. *Biogeosciences*, *12*, 4939–4951. wOS:000360294800005.

Bach, L. T., Mackinder, L. C. M., Schulz, K. G., Wheeler, G., Schroeder, D. C., Brownlee, C., & Riebesell, U. (2013). Dissecting the impact of CO_2 and pH on the mechanisms of photosynthesis and calcification in the coccolithophore Emiliania huxleyi. *New Phytologist*, *199*(1), 121–134. https://doi.org/10.1111/nph.12225

Bach, L. T., Riebesell, U., Gutowska, M. A., Federwisch, L., & Schulz, K. G. (2015). A unifying concept of coccolithophore sensitivity to changing carbonate chemistry embedded in an ecological framework. *Progress in Oceanography*, *135*, 125–138. https://doi.org/10.1016/j.pocean.2015.04.012

Balch, W. M., Bates, N. R., Lam, P. J., Twining, B. S., Rosengard, S. Z., Bowler, B. C., et al. (2016). Factors regulating the Great Calcite Belt in the Southern Ocean and its biogeochemical significance. *Global Biogeochemical Cycles*, *30*, 1124–1144. https://doi.org/10.1002/2016GB005414

Balch, W., Drapeau, D., Bowler, B., & Booth, E. (2007). Prediction of pelagic calcification rates using satellite measurements. *Deep Sea Research Part II: Topical Studies in Oceanography*, *54*(5–7), 478–495. https://doi.org/10.1016/j.dsr2.2006.12.006

Balch, W., Gordon, H. R., Bowler, B., Drapeau, D., & Booth, E. (2005). Calcium carbonate measurements in the surface global ocean based on moderate-resolution imaging spectroradiometer data. *Journal of Geophysical Research*, *110*, 1978–2012. https://doi.org/10.1029/2004JC002560

Barrett, P. M., Resing, J. A., Buck, N. J., Feely, R. A., Bullister, J. L., Buck, C. S., & Landing, W. M. (2014). Calcium carbonate dissolution in the upper 1000 m of the eastern North Atlantic. *Global Biogeochemical Cycles*, *28*, 386–397. https://doi.org/10.1002/2013GB004619

Beaufort, L., Probert, I., de Garidel-Thoron, T., Bendif, E. M., Ruiz-Pino, D., Metzl, N., et al. (2011). Sensitivity of coccolithophores to carbonate chemistry and ocean acidification. *Nature*, *476*(7358), 80–83.

Behrenfeld, M. J., & Falkowski, P. G. (1997). Photosynthetic rates derived from satellite-based chlorophyll concentration. *Limnology and Oceanography*, *42*(1), 1–20. https://doi.org/10.4319/lo.1997.42.1.0001

Bolton, C. T., Hernández-Sánchez, M. T., Fuertes, M.-Á., González-Lemos, S., Abrevaya, L., Mendez-Vicente, A., et al. (2016). Decrease in coccolithophore calcification and CO_2 since the middle Miocene. *Nature Communications*, *7*, 10,284 EP–.

Broecker, W., & Clark, E. (2009). Ratio of coccolith $CaCO_3$ to foraminifera $CaCO_3$ in late Holocene deep sea sediments. *Paleoceanography*, *24*, pA3205. https://doi.org/10.1029/2009PA001731

Buitenhuis, E. T., Vogt, M., Moriarty, R., Bednaršek, N., Doney, S. C., Leblanc, K., et al. (2013). MAREDAT: Towards a world atlas of marine ecosystem data. *Earth System Science Data*, *5*(2), 227–239. https://doi.org/10.5194/essd-5-227-2013

Daniels, C. J., Poulton, A. J., Balch, W. M., Marañón, E., Adey, T., Bowler, B. C., et al. (2018). A global compilation of coccolithophore calcification rates. *Earth System Science Data Discussions*, *2018*, 1–29. https://doi.org/10.5194/essd-2018-52

Davis, C. V., Rivest, E. B., Hill, T. M., Gaylord, B., Russell, A. D., & Sanford, E. (2017). Ocean acidification compromises a planktic calcifier with implications for global carbon cycling. *Scientific Reports*, *7*, 2225. https://doi.org/10.1038/s41598-017-01530-9

Dutkiewicz, S., Morris, J. J., Follows, M. J., Scott, J., Levitan, O., Dyhrman, S. T., & Berman-Frank, I. (2015). Impact of ocean acidification on the structure of future phytoplankton communities. *Nature Climate Change*, *5*, 1002–1006.

Fay, A. R., & McKinley, G. A. (2014). Global open-ocean biomes: Mean and temporal variability. *Earth System Science Data*, *6*(2), 273–284. https://doi.org/10.5194/essd-6-273-2014

Feely, R. A., Sabine, C. L., Lee, K., Berelson, W., Kleypas, J., Fabry, V. J., & Millero, F. J. (2004). Impact of anthropogenic CO_2 on the $CaCO_3$ system in the oceans. *Science*, *305*(5682), 362–366. https://doi.org/10.1126/science.1097329

Feng, Y., Hare, C., Leblanc, K., Rose, J. M., Zhang, Y., DiTullio, G. R., et al. (2009). Effects of increased pCO_2 and temperature on the North Atlantic spring bloom. I. The phytoplankton community and biogeochemical response. *Marine Ecology Progress Series*, *388*, 13–25.

Fielding, S. R. (2013). Emiliania huxleyi specific growth rate dependence on temperature. *Limnology and Oceanography*, *58*(2), 663–666. https://doi.org/10.4319/lo.2013.58.2.0663

Findlay, H. S., Calosi, P., & Crawfurd, K. (2011). Determinants of the PIC:POC response in the coccolithophore Emiliania huxleyi under future ocean acidification scenarios. *Limnology and Oceanography*, *56*(3), 1168–1178. https://doi.org/10.4319/lo.2011.56.3.1168

Freeman, N. M., & Lovenduski, N. S. (2015). Decreased calcification in the Southern Ocean over the satellite record. *Geophysical Research Letters*, *42*, 1834–1840. https://doi.org/10.1002/2014GL062769

Fu, W., Randerson, J. T., & Moore, J. K. (2016). Climate change impacts on net primary production (NPP) and export production (EP) regulated by increasing stratification and phytoplankton community structure in the CMIP5 models. *Biogeosciences*, *13*(18), 5151–5170. https://doi.org/10.5194/bg-13-5151-2016

Furukawa, M., Sato, T., Suzuki, Y., Casareto, B. E., & Hirabayashi, S. (2018). Numerical modelling of physiological and ecological impacts of ocean acidification on coccolithophores. *Journal of Marine Systems*, *182*, 12–30. https://doi.org/10.1016/j.jmarsys.2018.02.008

Gangstø, R., Gehlen, M., Schneider, B., Bopp, L., Aumont, O., & Joos, F. (2008). Modeling the marine aragonite cycle: Changes under rising carbon dioxide and its role in shallow water $CaCO_3$ dissolution. *Biogeosciences*, *5*(4), 1057–1072. https://doi.org/10.5194/bg-5-1057-2008

Gangstø, R., Joos, F., & Gehlen, M. (2011). Sensitivity of pelagic calcification to ocean acidification. *Biogeosciences*, *8*(2), 433–458. https://doi.org/10.5194/bg-8-433-2011

Gehlen, M., Gangstø, R., Schneider, B., Bopp, L., Aumont, O., & Ethe, C. (2007). *The fate of pelagic $CaCO_3$, production in a high CO_2 ocean: A model study, Biogeosciences*, *4*(4), 505–519. https://doi.org/10.5194/bg-4-505-2007

Gibbs, S. J., Bown, P. R., Ridgwell, A., Young, J. R., Poulton, A. J., & O'Dea, S. A. (2016). Ocean warming, not acidification, controlled coccolithophore response during past greenhouse climate change. *Geology*, *44*(1), 59. https://doi.org/10.1130/G37273.1

Gregg, W. W., & Casey, N. W. (2007). Modeling coccolithophores in the global oceans. *Deep Sea Research Part II: Topical Studies in Oceanography*, *54*(5–7), 447–477. https://doi.org/10.1016/j.dsr2.2006.12.007, the Role of Marine Organic Carbon and Calcite Fluxes in Driving Global Climate Change, Past and Future.

Hannisdal, B., Henderiks, J., & Liow, L. H. (2012). Long-term evolutionary and ecological responses of calcifying phytoplankton to changes in atmospheric CO_2. *Global Change Biology*, *18*(12), 3504–3516. https://doi.org/10.1111/gcb.12007

Heinze, C. (2004). Simulating oceanic $CaCO_3$ export production in the greenhouse. *Geophysical Research Letters*, *31*, L16308. https://doi.org/10.1029/2004GL020613

Henderiks, J., & Rickaby, R. E. M. (2007). A coccolithophore concept for constraining the cenozoic carbon cycle. *Biogeosciences*, *4*(3), 323–329. https://doi.org/10.5194/bg-4-323-2007

Holligan, P., Charalampopoulou, A., & Hutson, R. (2010). Seasonal distributions of the coccolithophore, Emiliania huxleyi, and of particulate inorganic carbon in surface waters of the Scotia Sea. *Journal of Marine Systems*, *82*(4), 195–205. https://doi.org/10.1016/j.jmarsys.2010.05.007

Hopkins, J., & Balch, W. M. (2018). A new approach to estimating coccolithophore calcification rates from space. *Journal of Geophysical Research: Biogeosciences*, *123*, 1447–1459. https://doi.org/10.1002/2017JG004235

Hopkins, J., Henson, S. A., Painter, S. C., Tyrrell, T., & Poulton, A. J. (2015). Phenological characteristics of global coccolithophore blooms. *Global Biogeochemical Cycles*, *29*, 239–253. https://doi.org/10.1002/2014GB004919

Iglesias-Rodriguez, M. D., Armstrong, R., Feely, R., Hood, R., Kleypas, J., Milliman, J. D., et al. (2002). Progress made in study of ocean's calcium carbonate budget. *Eos Transactions American Geophysical Union*, *83*(34), 365–375. https://doi.org/10.1029/2002EO000267

Iglesias-Rodriguez, M. D., Halloran, P. R., Rickaby, R. E. M., Hall, I. R., Colmenero-Hidalgo, E., Gittins, J. R., et al. (2008). Phytoplankton calcification in a high-CO_2 world. *Science*, *320*(5874), 336–340. https://doi.org/10.1126/science.1154122

Irwin, A. J., & Finkel, Z. V. (2018). Microbial Ecology of the Oceans, *Phytoplankton functional types: A trait perspective* (pp. 528). Hoboken, NJ: John Wiley and Sons Inc.

Jin, X., Gruber, N., Dunne, J. P., Sarmiento, J. L., & Armstrong, R. A. (2006). Diagnosing the contribution of phytoplankton functional groups to the production and export of particulate organic carbon, $CaCO_3$, and opal from global nutrient and alkalinity distributions. *Global Biogeochemical Cycles*, *20*, GB2015. https://doi.org/10.1029/2005GB002532

Krumhardt, K. M., Lovenduski, N. S., Freeman, N. M., & Bates, N. R. (2016). Apparent increase in coccolithophore abundance in the subtropical North Atlantic from 1990 to 2014. *Biogeosciences*, *13*(4), 1163–1177. https://doi.org/10.5194/bg-13-1163-2016

Krumhardt, K. M., Lovenduski, N. S., Iglesias-Rodriguez, M. D., & Kleypas, J. A. (2017a). Coccolithophore growth and calcification in a changing ocean. *Progress in Oceanography*, *159*, 276–295. https://doi.org/10.1016/j.pocean.2017.10.007

Krumhardt, K. M., Lovenduski, N. S., Long, M. C., & Lindsay, K. (2017b). Avoidable impacts of ocean warming on marine primary production: Insights from the CESM ensembles. *Global Biogeochemical Cycles*, *31*, 114–133. https://doi.org/10.1002/2016GB005528

Kvale, K. F., Meissner, K. J., & Keller, D. P. (2015b). Potential increasing dominance of heterotrophy in the global ocean. *Environmental Research Letters*, *10*(7), 074009.

Kvale, K. F., Meissner, K. J., Keller, D. P., Eby, M., & Schmittner, A. (2015a). Explicit planktic calcifiers in the University of Victoria Earth System Climate Model, version 2.9. *Atmosphere-Ocean*, *53*(3), 332–350. https://doi.org/10.1080/07055900.2015.1049112

Large, W., & Yeager, S. (2004). Diurnal to decadal global forcing for ocean and sea-ice models: The data sets and flux climatologies (NCAR technical note: NCAR/TN-460+STR). Boulder, CO: CGD Division of the National Center for Atmospheric Research.

Laufkötter, C., Vogt, M., Gruber, N., Aumont, O., Bopp, L., Doney, S. C., et al. (2016). Projected decreases in future marine export production: The role of the carbon flux through the upper ocean ecosystem. *Biogeosciences*, *13*(13), 4023–4047. https://doi.org/10.5194/bg-13-4023-2016

Lauvset, S. K., Key, R. M., Olsen, A., van Heuven, S., Velo, A., Lin, X., et al. (2016). A new global interior ocean mapped climatology: The 1°x1° GLODAP version 2. *Earth System Science Data*, *8*, 325–340. https://doi.org/10.5194/essd-8-325-2016

Lee, K. (2001). Global net community production estimated from the annual cycle of surface water total dissolved inorganic carbon. *Limnology and Oceanography*, *46*(6), 1287–1297. https://doi.org/10.4319/lo.2001.46.6.1287

Letscher, R. T., Moore, J. K., Teng, Y.-C., & Primeau, F. (2015). Variable C:N:P stoichiometry of dissolved organic matter cycling in the Community Earth System Model. *Biogeosciences*, *12*(1), 209–221. https://doi.org/10.5194/bg-12-209-2015

Locarnini, R. A., Mishonov, A. V., Antonov, J. I., Boyer, T. P., Garcia, H. E., Baranova, O. K., et al. (2013). World Ocean Atlas 2013, volume 1: Temperature. NOAA Atlas NESDIS 73.

Lohbeck, K. T., Riebesell, U., & Reusch, T. B. H. (2012). Adaptive evolution of a key phytoplankton species to ocean acidification. *Nature Geoscience*, *5*, 346 EP–.

Lovenduski, N. S., Gruber, N., Doney, S. C., & Lima, I. D. (2007). Enhanced CO_2 outgassing in the Southern Ocean from a positive phase of the Southern Annular Mode. *Global Biogeochemical Cycles*, *21*, GB2026. https://doi.org/10.1029/2006GB002900

Marañón, E., Balch, W. M., Cermeño, P., González, N., Sobrino, C., Fernández, A., et al. (2016). Coccolithophore calcification is independent of carbonate chemistry in the tropical ocean. *Limnology and Oceanography*, *61*(4), 1345–1357. https://doi.org/10.1002/lno.10295

Milliman, J. D. (1993). Production and accumulation of calcium carbonate in the ocean: Budget of a nonsteady state. *Global Biogeochemical Cycles*, *7*(4), 927–957. https://doi.org/10.1029/93GB02524

Milliman, J., Troy, P., Balch, W., Adams, A., Li, Y.-H., & Mackenzie, F. (1999). Biologically mediated dissolution of calcium carbonate above the chemical lysocline? *Deep Sea Research Part I: Oceanographic Research Papers*, *46*(10), 1653–1669. https://doi.org/10.1016/S0967-0637(99)00034-5

Monteiro, F. M., Bach, L. T., Brownlee, C., Bown, P., Rickaby, R. E. M., Poulton, A. J., et al. (2016). Why marine phytoplankton calcify. *Science Advances*, *2*(7), e1501822. https://doi.org/10.1126/sciadv.1501822

Moore, J., Doney, S. C., Kleypas, J. A., Glover, D. M., & Fung, I. Y. (2002). An intermediate complexity marine ecosystem model for the global domain. *Deep Sea Research Part II: Topical Studies in Oceanography*, *49*(1), 403–462. https://doi.org/10.1016/S0967-0645(01)00108-4, the US JGOFS Synthesis and Modeling Project: Phase 1.

Moore, J. K., Doney, S. C., & Lindsay, K. (2004). Upper ocean ecosystem dynamics and iron cycling in a global three-dimensional model. *Global Biogeochemical Cycles*, *18*, GB4028. https://doi.org/10.1029/2004GB002220

Moore, J. K., Lindsay, K., Doney, S. C., Long, M. C., & Misumi, K. (2013). Marine ecosystem dynamics and biogeochemical cycling in the community earth system model [CESM1(BGC)]: Comparison of the 1990s with the 2090s under the RCP4.5 and RCP8.5 scenarios. *Journal of Climate*, *26*(23), 9291–9312. https://doi.org/10.1175/JCLI-D-12-00566.1

Moy, A. D., Howard, W. R., Bray, S. G., & Trull, T. W. (2009). Reduced calcification in modern southern ocean planktonic foraminifera. *Nature Geoscience*, *2*, 276–280.

Müller, M. N., Trull, T., & Hallegraeff, G. (2015). Differing responses of three southern ocean Emiliania huxleyi ecotypes to changing seawater carbonate chemistry. *Marine Ecology Progress Series*, *531*, 81–90.

Nissen, C., Vogt, M., Münnich, M., Gruber, N., & Haumann, F. A. (2018). Factors controlling coccolithophore biogeography in the Southern Ocean. *Biogeosciences*, *15*(22), 6997–7024. https://doi.org/10.5194/bg-15-6997-2018

O'Brien, C. J., Peloquin, J. A., Vogt, M., Heinle, M., Gruber, N., Ajani, P., et al. (2013). Global marine plankton functional type biomass distributions: Coccolithophores. *Earth System Science Data*, *5*(2), 259–276. https://doi.org/10.5194/essd-5-259-2013

O'Brien, C. J., Vogt, M., & Gruber, N. (2016). Global coccolithophore diversity: Drivers and future change. *Progress in Oceanography*, *140*, 27–42. https://doi.org/10.1016/j.pocean.2015.10.003

Olson, M., & Strom, S. L. (2002). Phytoplankton growth, microzooplankton herbivory and community structure in the southeast Bering Sea: Insight into the formation and temporal persistence of an Emiliania huxleyi bloom. *Deep Sea Research Part II: Topical Studies in Oceanography*, *49*(26), 5969–5990. https://doi.org/10.1016/S0967-0645(02)00329-6, ecology of the SE Bering Sea.

Orr, J. C., Fabry, V. J., Aumont, O., Bopp, L., Doney, S. C., Feely, R. A., et al. (2005). Anthropogenic ocean acidification over the twenty-first century and its impact on calcifying organisms. *Nature*, *437*(7059), 681–686.

Paasche, E. (1973). Silicon and the ecology of marine plankton diatoms. II. Silicate-uptake kinetics in five diatom species. *Marine Biology*, *19*(3), 262–269. https://doi.org/10.1007/BF02097147

Pinsonneault, A. J., Matthews, H. D., Galbraith, E. D., & Schmittner, A. (2012). Calcium carbonate production response to future ocean warming and acidification. *Biogeosciences*, *9*(6), 2351–2364. https://doi.org/10.5194/bg-9-2351-2012

Poulton, A. J., Adey, T. R., Balch, W. M., & Holligan, P. M. (2007). Relating coccolithophore calcification rates to phytoplankton community dynamics: Regional differences and implications for carbon export. *Deep Sea Research Part II: Topical Studies in Oceanography*, *54*(5–7), 538–557. https://doi.org/10.1016/j.dsr2.2006.12.003, the Role of Marine Organic Carbon and Calcite Fluxes in Driving Global Climate Change, Past and Future.

Poulton, A. J., Holligan, P. M., Charalampopoulou, A., & Adey, T. R. (2017). Coccolithophore ecology in the tropical and subtropical Atlantic Ocean: New perspectives from the Atlantic meridional transect (AMT) programme. *Progress in Oceanography*, *158*, 150–170. https://doi.org/10.1016/j.pocean.2017.01.003

Ridgwell, A., Schmidt, D. N., Turley, C., Brownlee, C., Maldonado, M. T., Tortell, P., & Young, J. R. (2009). From laboratory manipulations to Earth System Models: Scaling calcification impacts of ocean acidification. *Biogeosciences*, *6*(11), 2611–2623. https://doi.org/10.5194/bg-6-2611-2009

Ridgwell, A., Zondervan, I., Hargreaves, J. C., Bijma, J., & Lenton, T. M. (2007). Assessing the potential long-term increase of oceanic fossil fuel CO_2 uptake due to CO_2-calcification feedback. *Biogeosciences*, *4*(4), 481–492. https://doi.org/10.5194/bg-4-481-2007

Riebesell, U. (2004). Effects of CO_2 enrichment on marine phytoplankton. *Journal of Oceanography*, *60*(4), 719–729. https://doi.org/10.1007/s10872-004-5764-z

Riebesell, U., Zondervan, I., Rost, B., Tortell, P. D., Zeebe, R. E., & Morel, F. M. M. (2000). Reduced calcification of marine plankton in response to increased atmospheric CO_2. *Nature*, *407*(6802), 364–367.

Rivero-Calle, S., Gnanadesikan, A., Del Castillo, C. E., Balch, W. M., & Guikema, S. D. (2015). Multidecadal increase in North Atlantic coccolithophores and the potential role of rising CO_2. *Science*, *350*(6267), 1533–1537. https://doi.org/10.1126/science.aaa8026

Rost, B., Riebesell, U., Burkhardt, S., & Sültemeyer, D. (2003). Carbon acquisition of bloom-forming marine phytoplankton. *Limnology and Oceanography*, *48*(1), 55–67. https://doi.org/10.4319/lo.2003.48.1.0055

Sarmiento, J. L., Dunne, J., Gnanadesikan, A., Key, R. M., Matsumoto, K., & Slater, R. (2002). A new estimate of the $CaCO_3$ to organic carbon export ratio. *Global Biogeochemical Cycles*, *16*(4), 1107. https://doi.org/10.1029/2002GB001919

Sarmiento, J. L., & Gruber, N. (2006). *Ocean biogeochemical dynamics*, pp. Princeton, Woodstock: Princeton University Press.

Sarthou, G., Timmermans, K. R., Blain, S., & Tréguer, P. (2005). Growth physiology and fate of diatoms in the ocean: A review. *Journal of Sea Research*, *53*(1), 25–42. https://doi.org/10.1016/j.seares.2004.01.007, iron Resources and Oceanic Nutrients - Advancement of Global Environmental Simulations.

Schiebel, R. (2002). Planktic foraminiferal sedimentation and the marine calcite budget. *Global Biogeochemical Cycles*, *16*(4), 1065. https://doi.org/10.1029/2001GB001459

Sett, S., Bach, L. T., Schulz, K. G., Koch-Klavsen, S., Lebrato, M., & Riebesell, U. (2014). Temperature modulates coccolithophorid sensitivity of growth, photosynthesis and calcification to increasing seawater pCO_2. *PLoS ONE*, *9*(2), E88308. https://doi.org/10.1371/journal.pone.0088308

Sherman, E., Moore, J. K., Primeau, F., & Tanouye, D. (2016). Temperature influence on phytoplankton community growth rates. *Global Biogeochemical Cycles*, *30*, 550–559. https://doi.org/10.1002/2015GB005272

Smith, S. V., & Mackenzie, F. T. (2016). The role of $CaCO_3$ reactions in the contemporary oceanic CO_2 cycle. *Aquatic Geochemistry*, *22*(2), 153–175. https://doi.org/10.1007/s10498-015-9282-y

Steele, M., Morley, R., Ermold, W., & 2079–2087 (2001). PHC: A global ocean hydrography with a high-quality Arctic Ocean. *Journal of Climate*, *14*(9). https://doi.org/10.1175/1520-0442(2001)014<2079:PAGOHW>2.0.CO;2

Thierstein, H. R., & Young, J. R. (2004). *Coccolithophores: From molecular processes to global impact*. Verlag Berlin Heidelberg: Springer Science & Business Media.

Winter, A., Henderiks, J., Beaufort, L., Rickaby, R. E. M., & Brown, C. W. (2013). Poleward expansion of the coccolithophore Emiliania huxleyi. *Journal of Plankton Research*, *36*, 316–325. https://doi.org/10.1093/plankt/fbt110